



State Key Laboratory of Numerical Modelling for Atmospheric Sciences
and Geophysical Fluid Dynamics(LASG)
Institute of Atmospheric Physics Chinese Academy of Sciences

Asian Monsoon in a Global Perspective

Tianjun ZHOU

zhoutj@lasg.iap.ac.cn

2nd ACAM Training School: Observation & modeling of atmospheric chemistry & aerosols in the Asian monsoon region

10-12 June 2017, Jinan University, Guangzhou China



Outline

1. Background

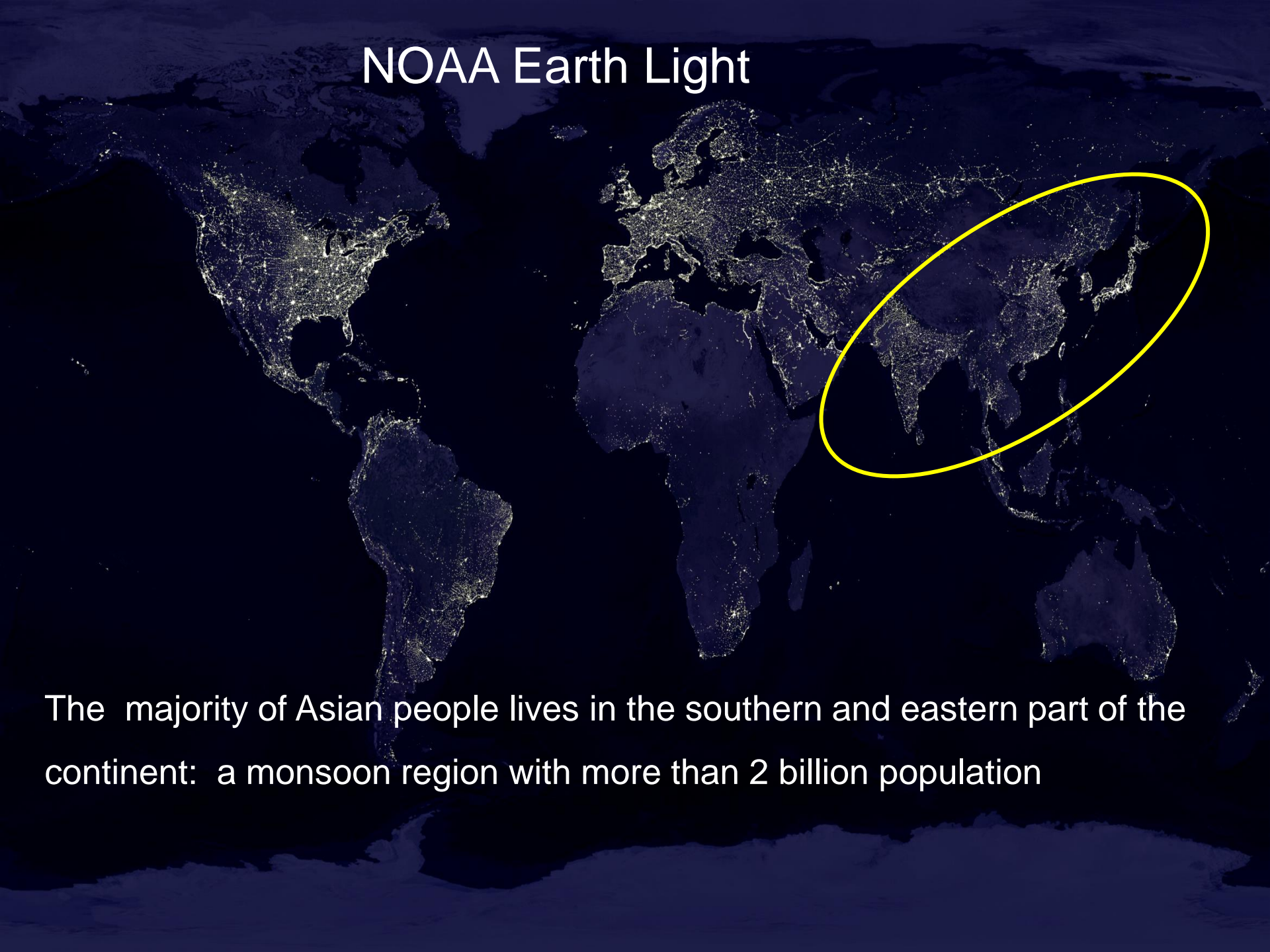
2. Overview of GM

3. Responses to external forcings

4. Concluding remarks

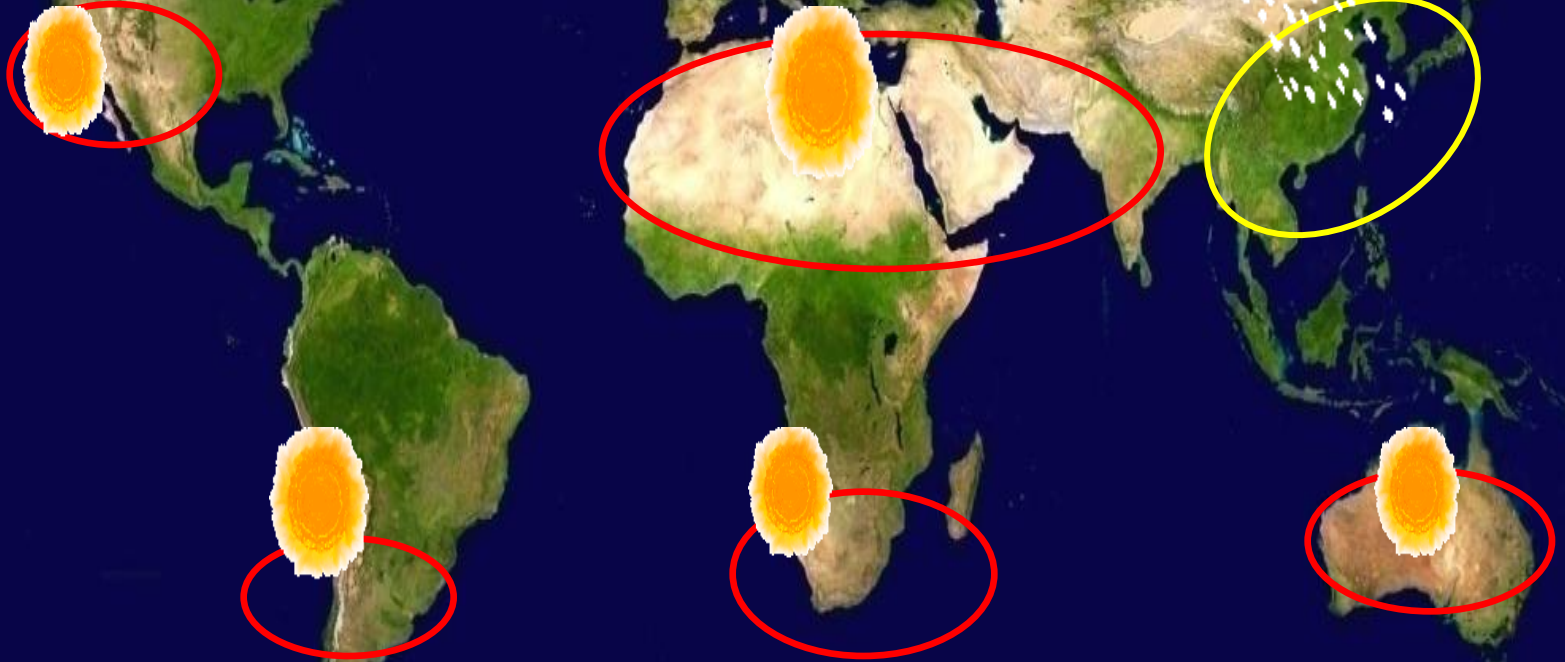


NOAA Earth Light



The majority of Asian people lives in the southern and eastern part of the continent: a monsoon region with more than 2 billion population

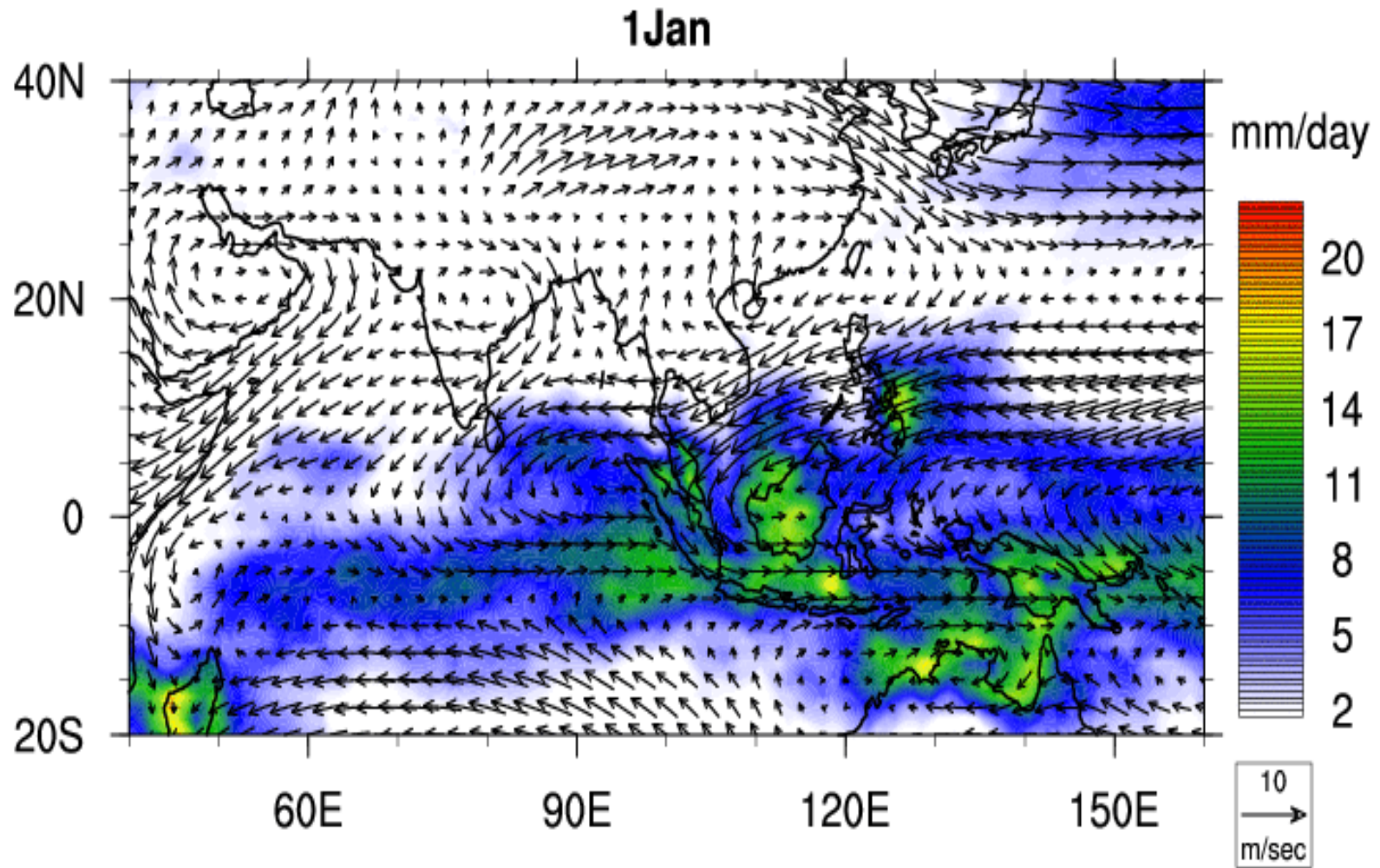
Monsoon in Asia: Supply of water resources for more than one billion people



Subtropical regions of the world are arid/semi-arid regions except for EA

Monsoon, manifested by wind & rainfall

Seasonal Migration of Tropical Convergence Zone (TCZ)



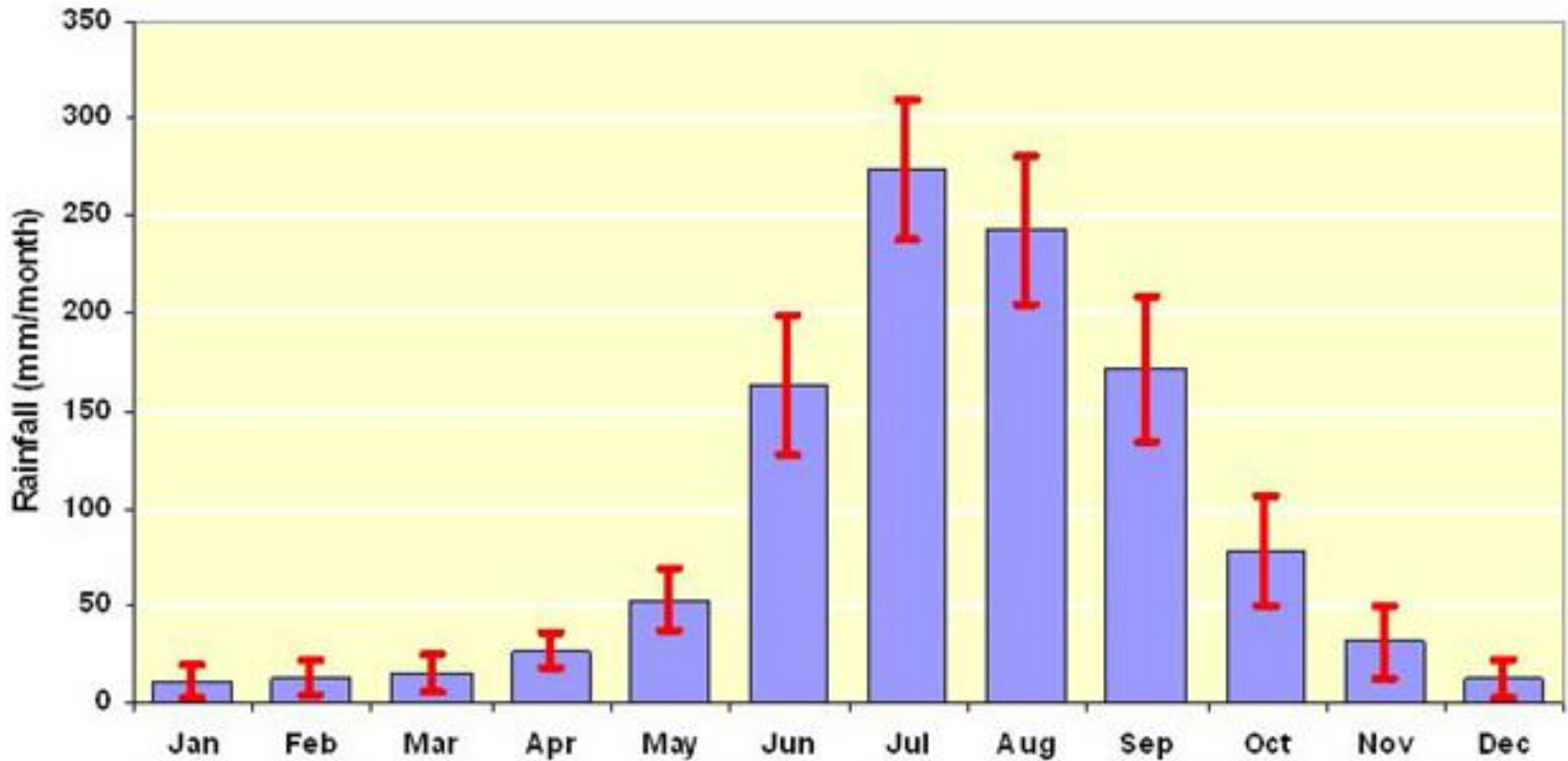
Annual evolution of daily mean Winds at 850 hPa and Precipitation

Courtesy: Roxy Mathew Koll

Monsoon, manifested by wind & rainfall



Seasonal Migration of Tropical Convergence Zone (TCZ)



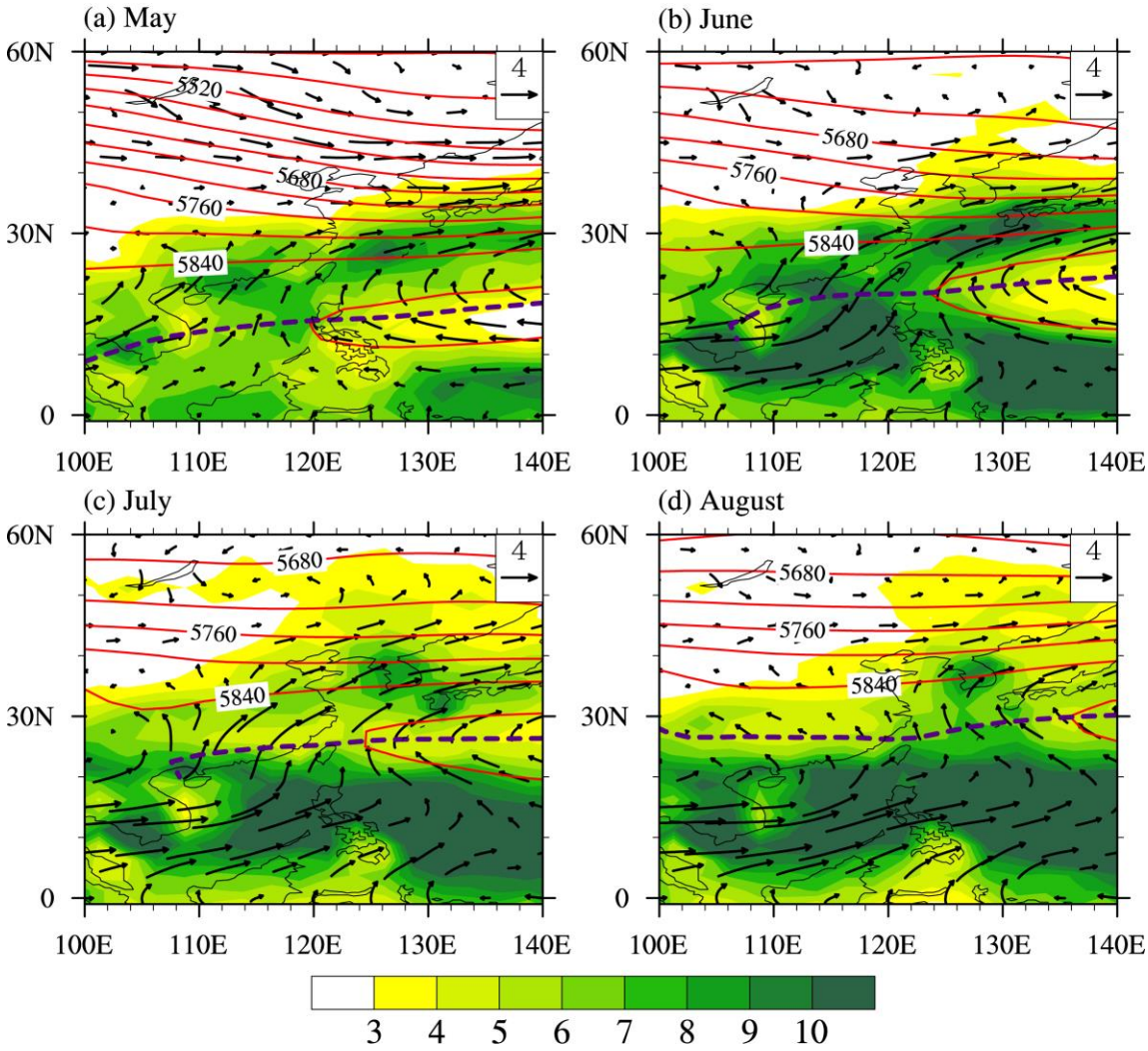
Annual cycle of Indian rainfall

Courtesy: Roxy Mathew Koll

East Asian monsoon: Tropical & subtropical parts due to the existence of WPSH



Mean Circulation (ERA40) and Rainfall



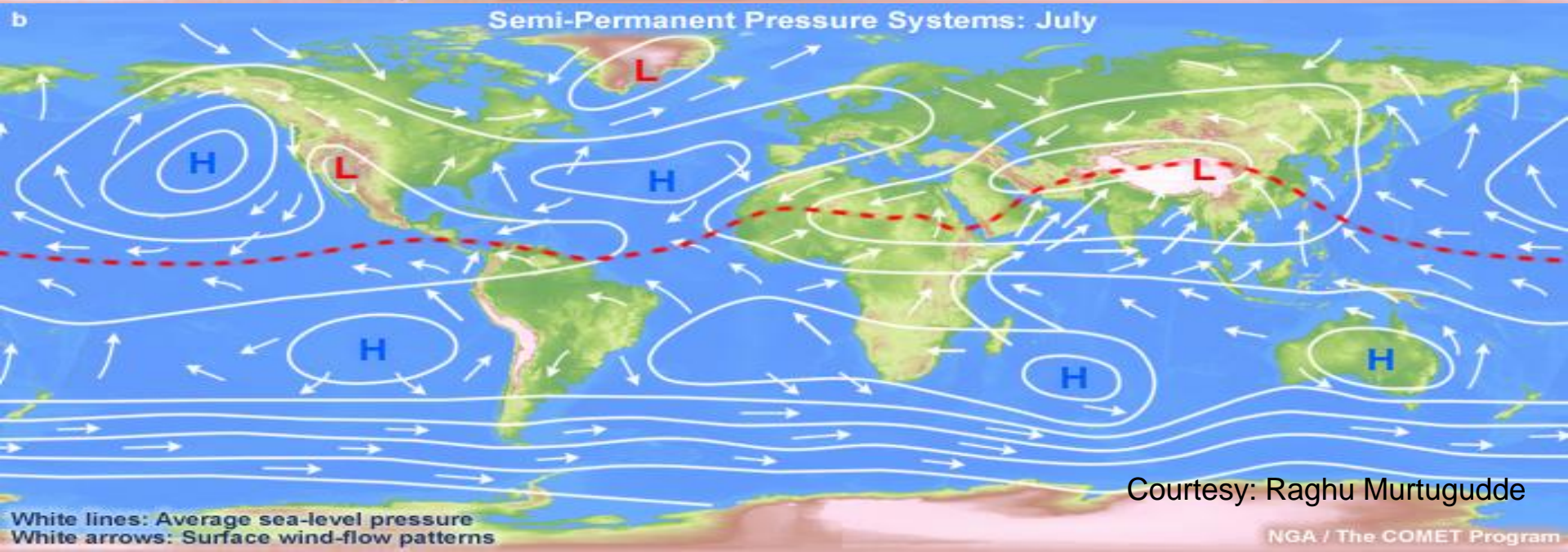
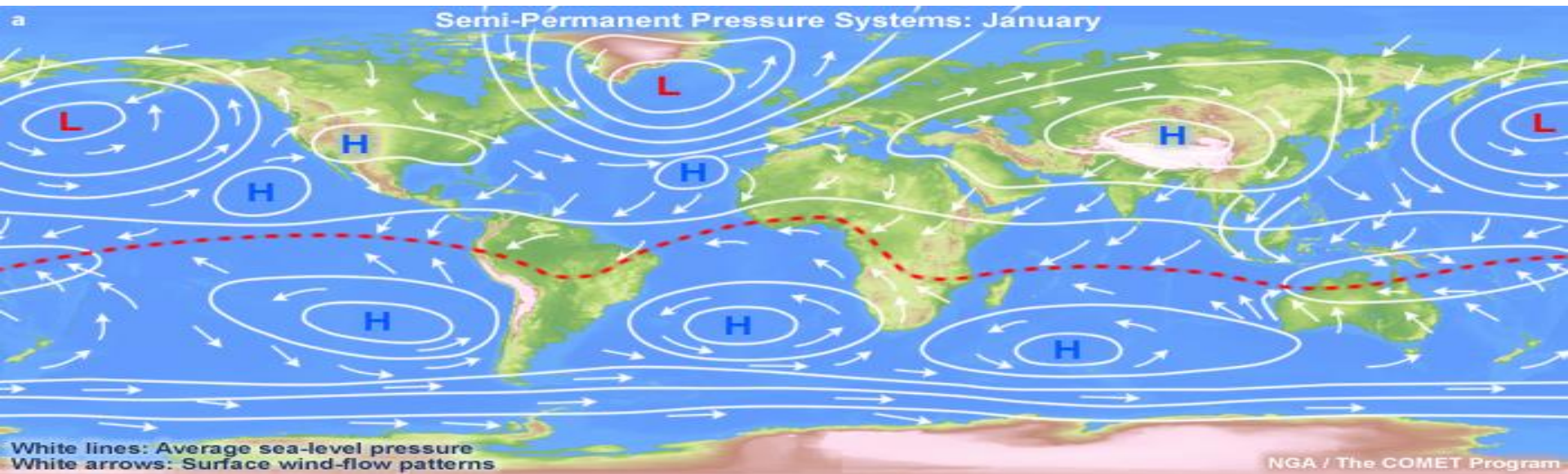
Zhou, T., D. Gong, J. Li, B. Li, 2009: Detecting and understanding the multi-decadal variability of the East Asian Summer Monsoon -- Recent progress and state of affairs. *Meteorologische Zeitschrift*, 18 (4), 455-467

Why are there monsoons?

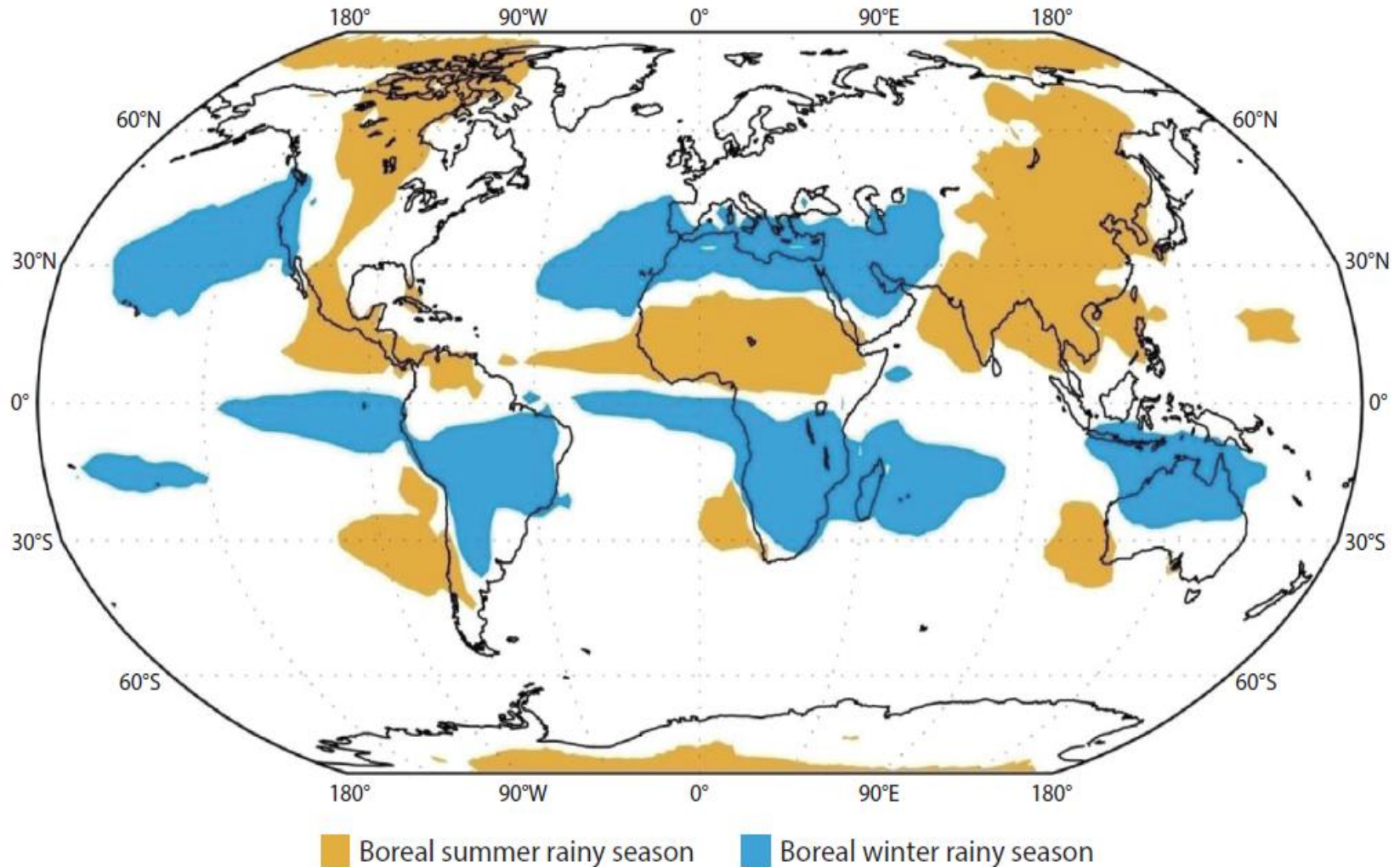
Monsoon Annual Cycle – Robust ?

- land-sea thermal contrast (Ts/Ps gradient)
- Orography (Tibet – elevated heat source)
(East Africa – frictional force
cross-equatorial flow)
- Earth's rotation (Coriolis force)
- Moisture from the tropical Indian Ocean

ITCZ – The Global Tropical Conveyor



We should obviously be able to relate the ITCZ to rainy seasons on land



Courtesy: Raghu Murtugudde

Mean Upper-Tropospheric Temperature: 200-500 mbar

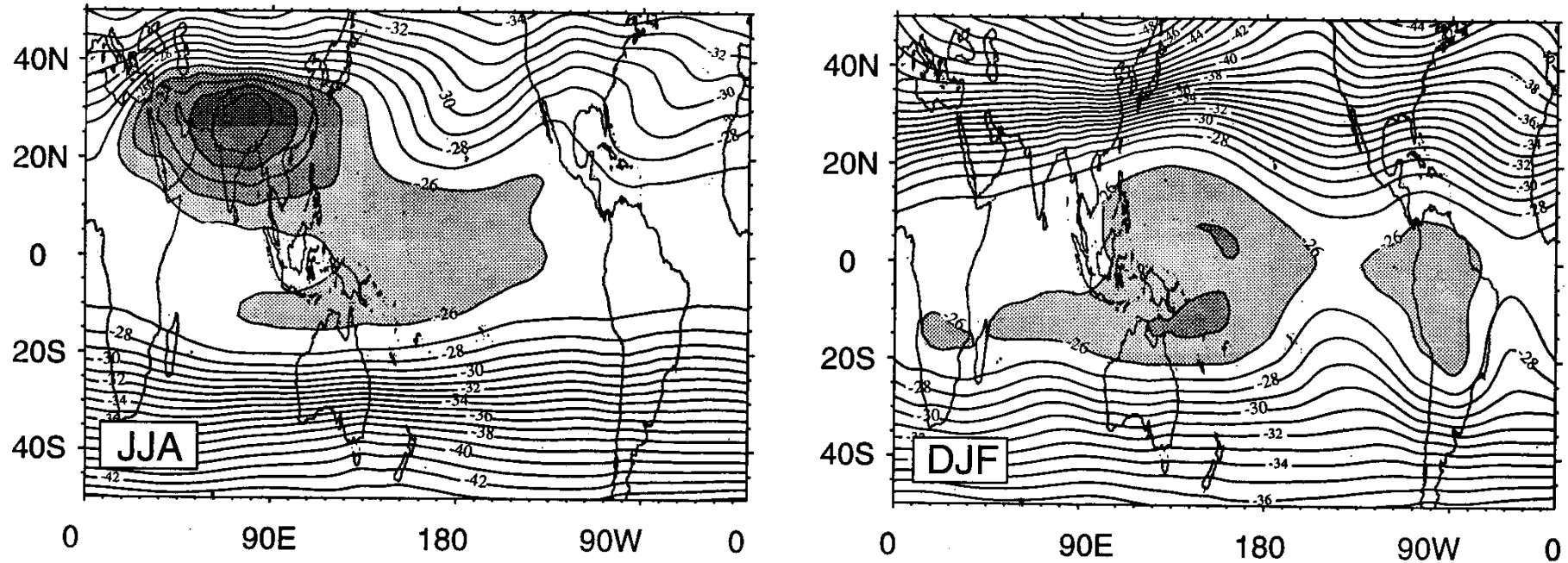
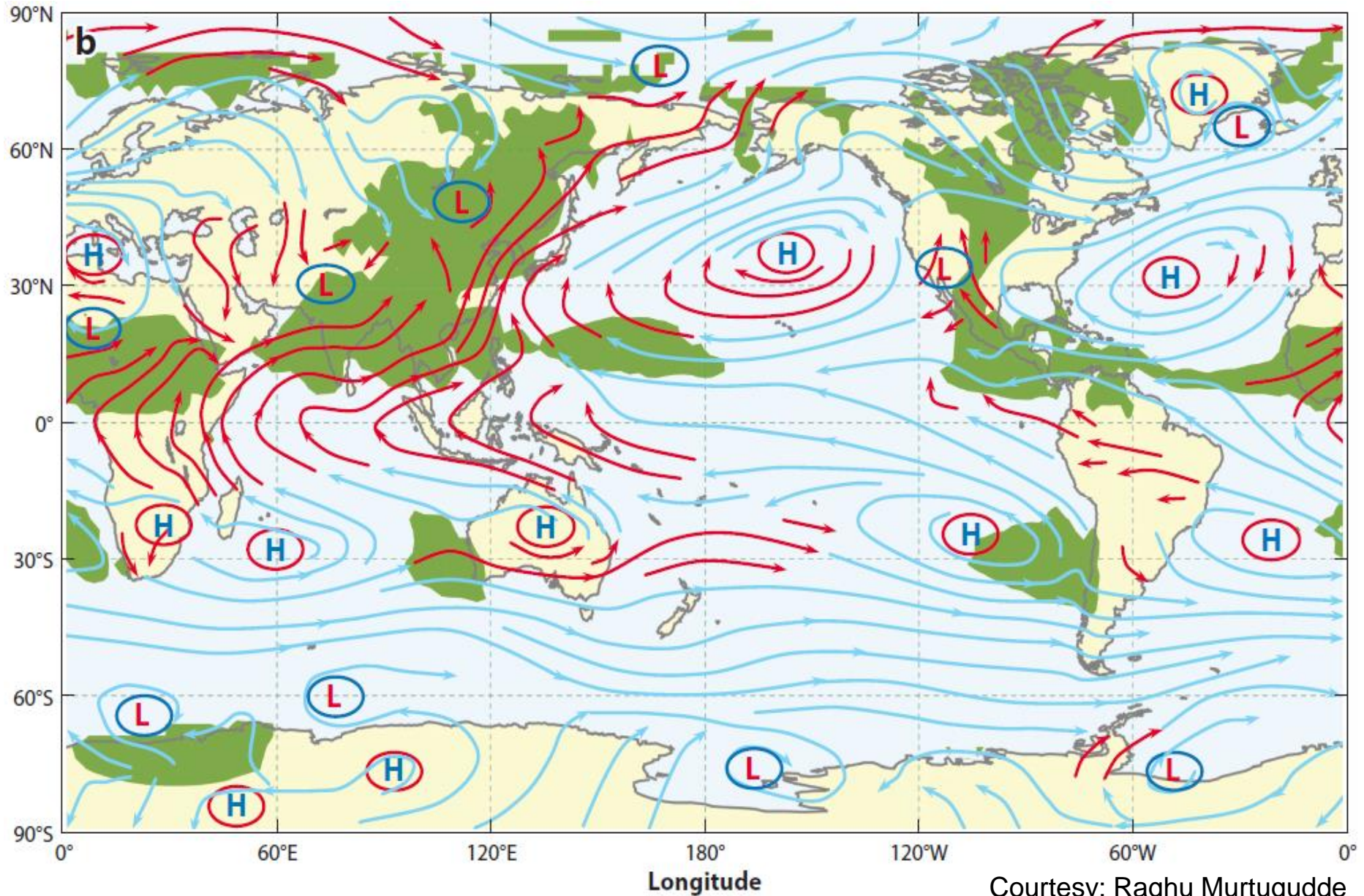


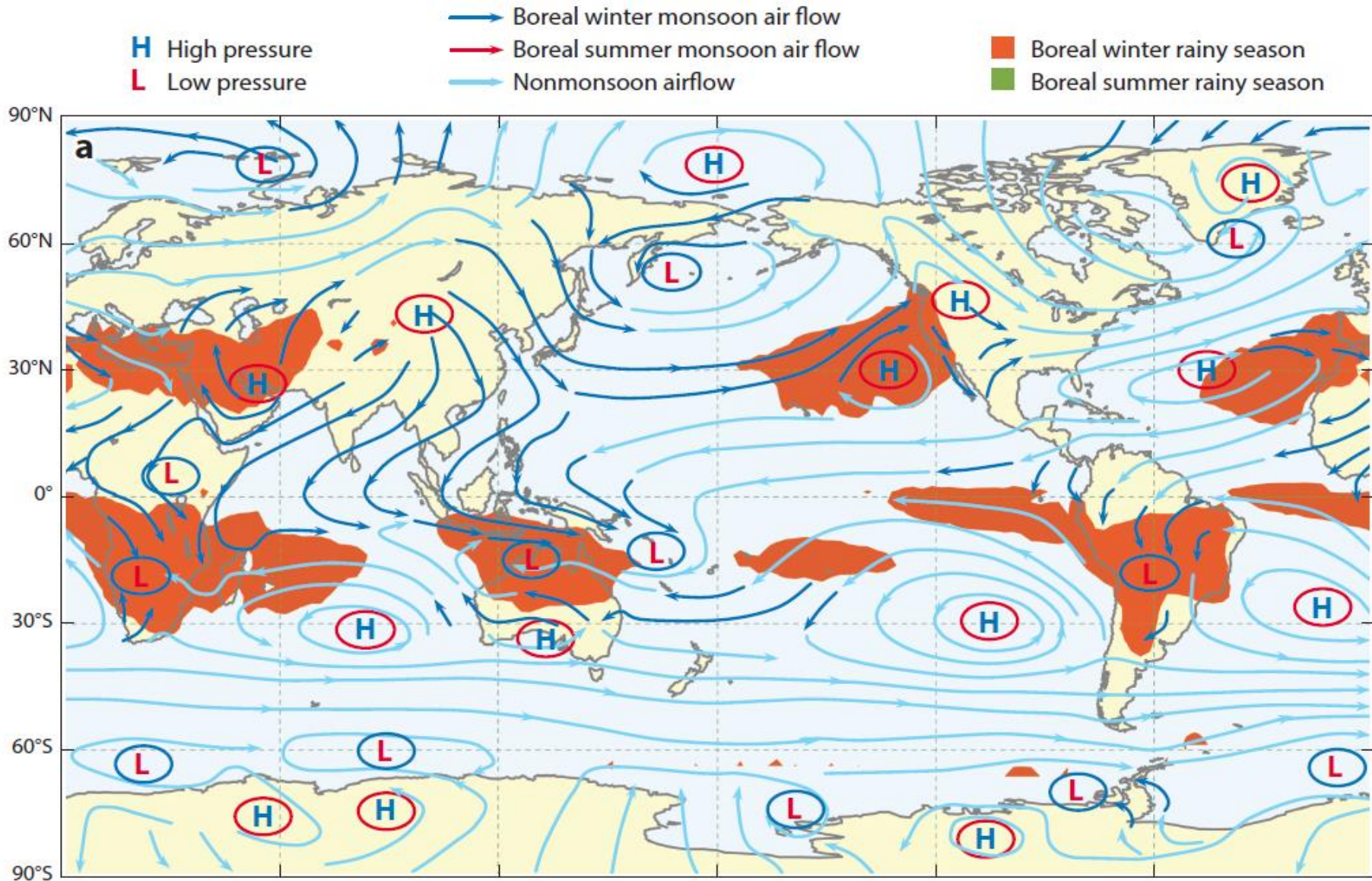
Figure 6a. Mean upper tropospheric (200–500 mbar) temperature (degrees Celsius) for the boreal summer (JJA), and boreal winter (DJF), averaged between 1979 and 1992. The boreal summer plot is based on calculations first made by *Li and Yanai* [1996]. Mean columnar temperatures warmer than -25°C are shaded.

Boreal Summer monsoon



Courtesy: Raghu Murtugudde

Boreal winter monsoon



Courtesy: Raghu Murtugudde

Indian Flood



© EPA

Indian Flood



Reuters

Pakistan Flood



<http://i.cdn.turner.com/cnn/interactive/2010/08/world/gallery.large.pakistan.flood>



Wuhan Railway Station

04 pm, 08 July, 2016

中新網
Chinanews.com

Extreme rainfall in Beijing: July 21, 2012

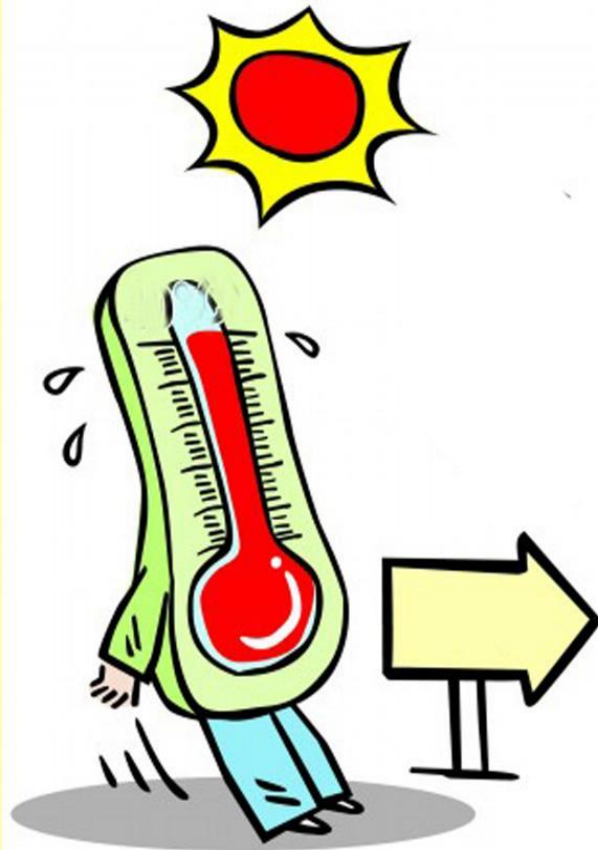


Beijing Subway

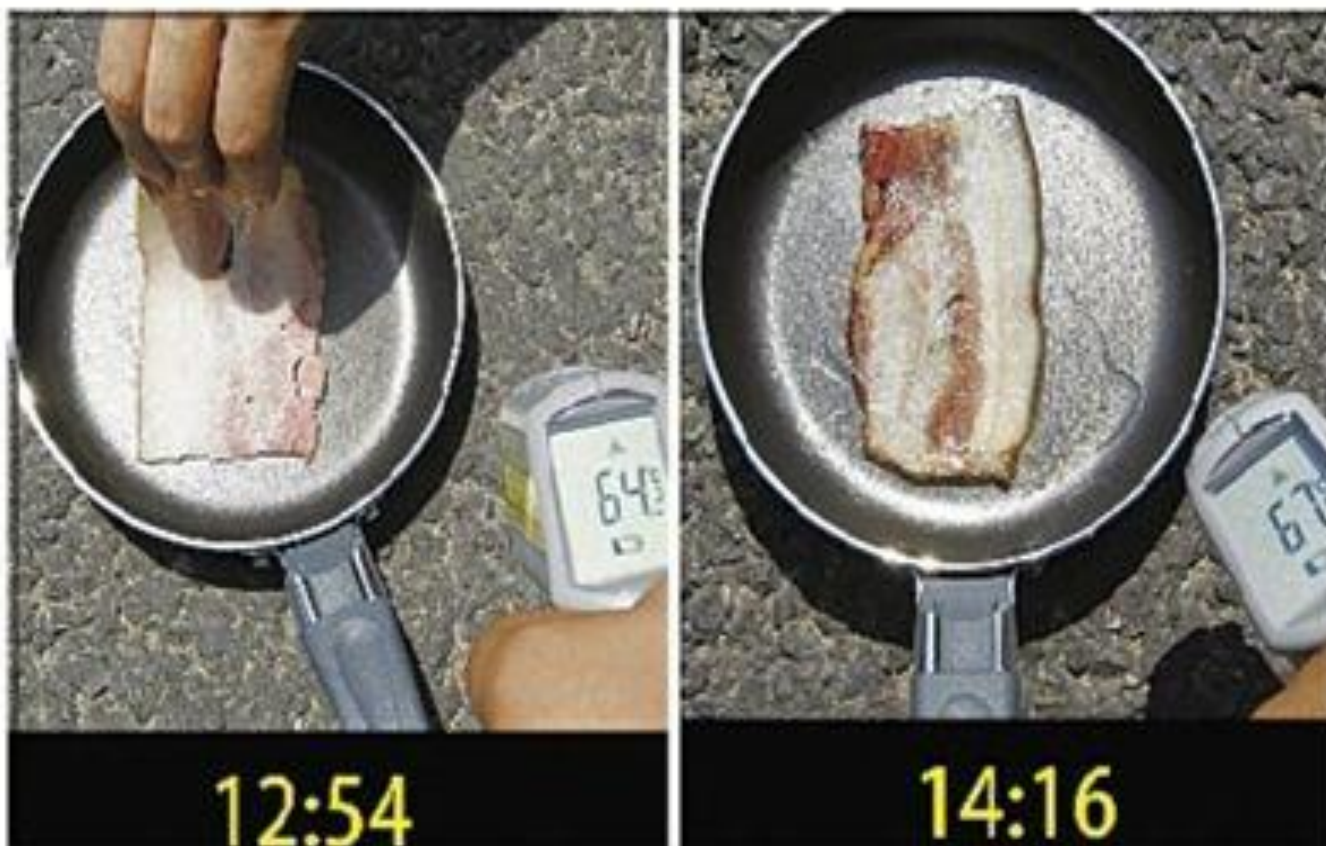


Northern suburb of Beijing

Heat Wave in China : Aug 2013



Heat Wave in China : Aug 2013



Shanghai

2008 Jan. cold surge and frozen disasters snowstorm in S. China



From Jan 10 to Jan 31, 2008:

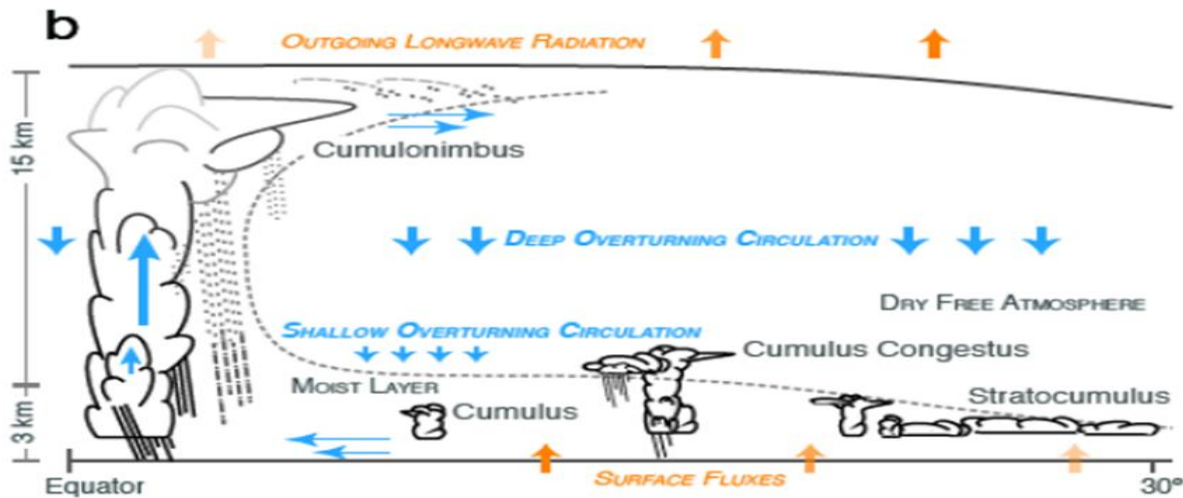
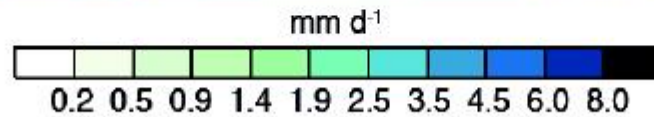
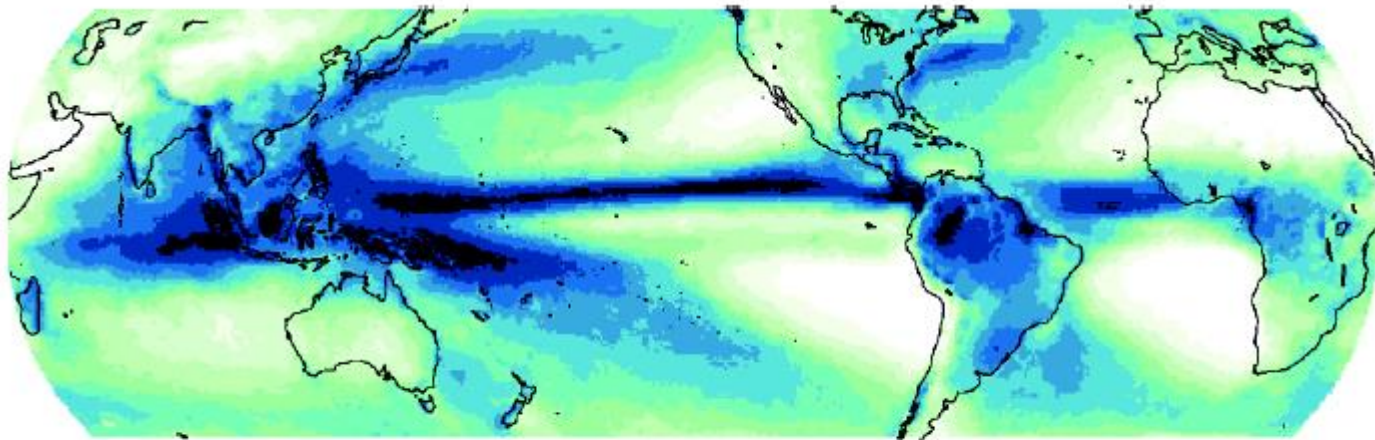
10 provinces affected, 60 people died.

Economic loss more than 53.79 billion RMB

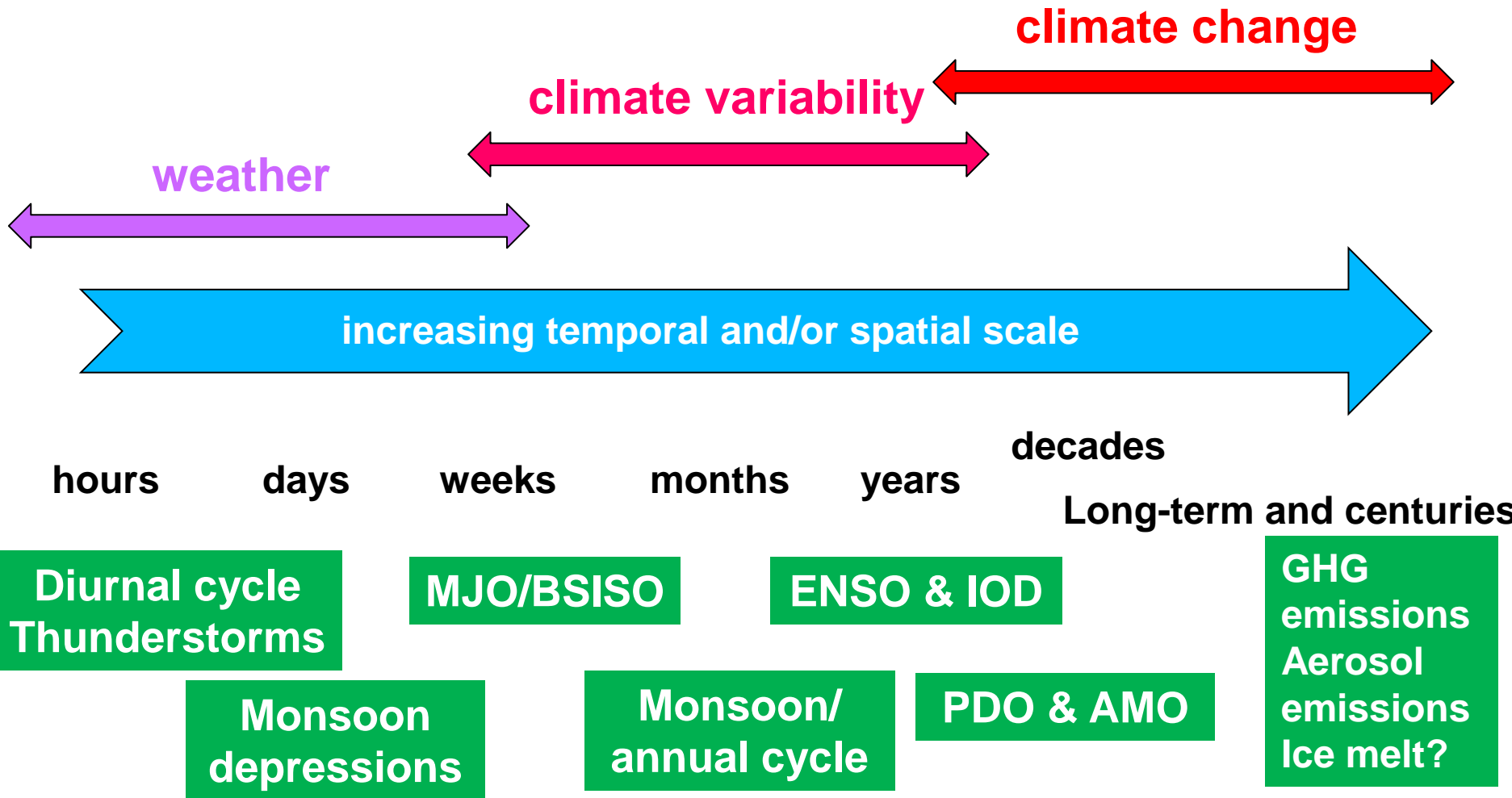
(6 RMB=1 USD)



Monsoon deep convection: S&T interaction, Cloud & Radiation feedback



Space and time scales in the monsoon





We focus on the monsoon responses to external forcing agents



Outline

1. Background

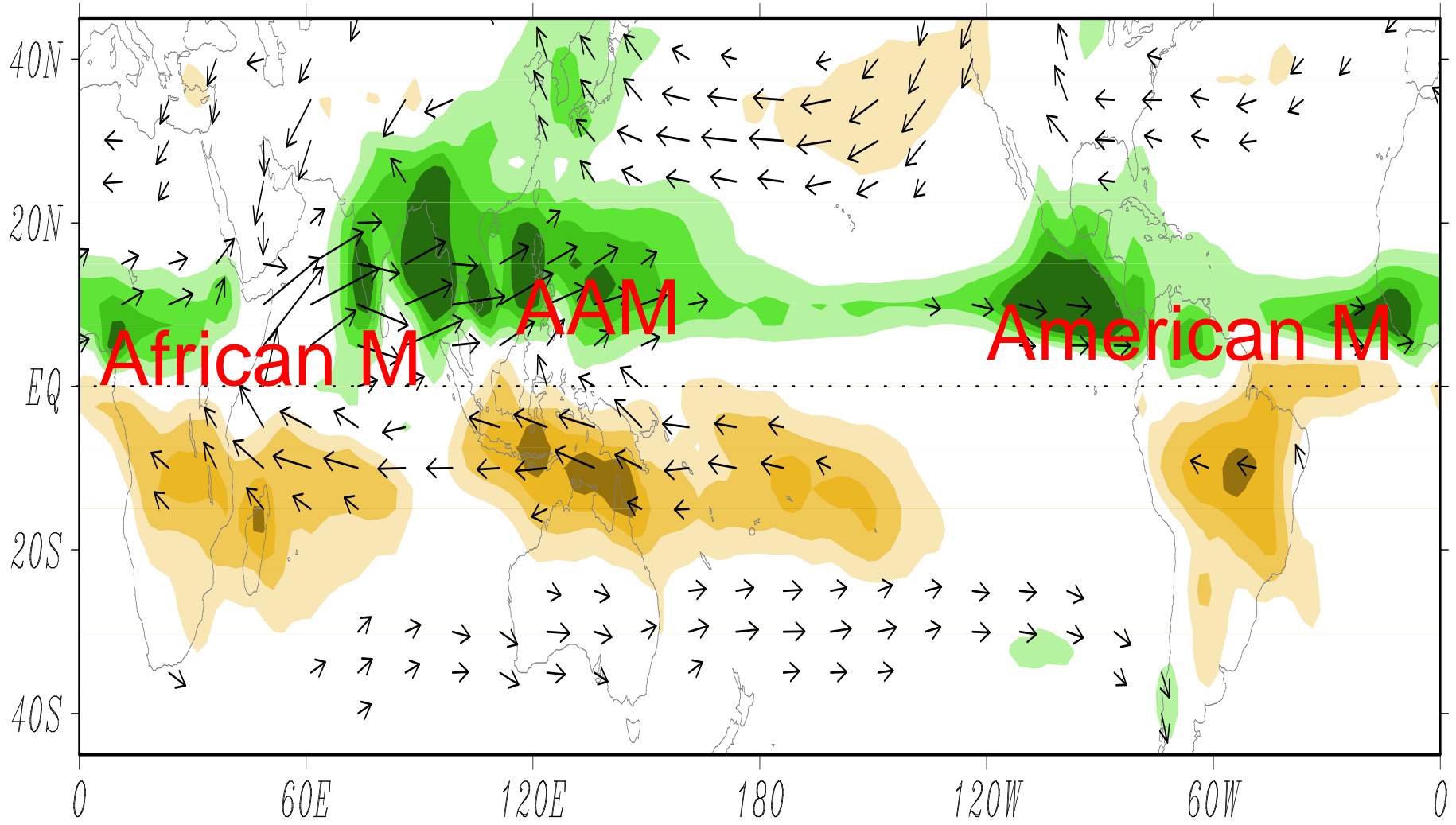
2. Overview of GM

3. Responses to external forcings

4. Concluding remarks



Global Monsoons



JJA –DJF UV850 & Precipitation

Monsoon Prec. Intensity and Domain



1. Monsoon Prec. Intensity:

(a) **Annual Range**: Local summer Minus Local Winter Prec.

AR (Annual Range) = $PR_{JJA} - PR_{DJF}$ (in North Hemisphere)

$PR_{DJF} - PR_{JJA}$ (in South Hemisphere)

(b) **Area averaged local summer Pr at each grid within the present monsoon domain**

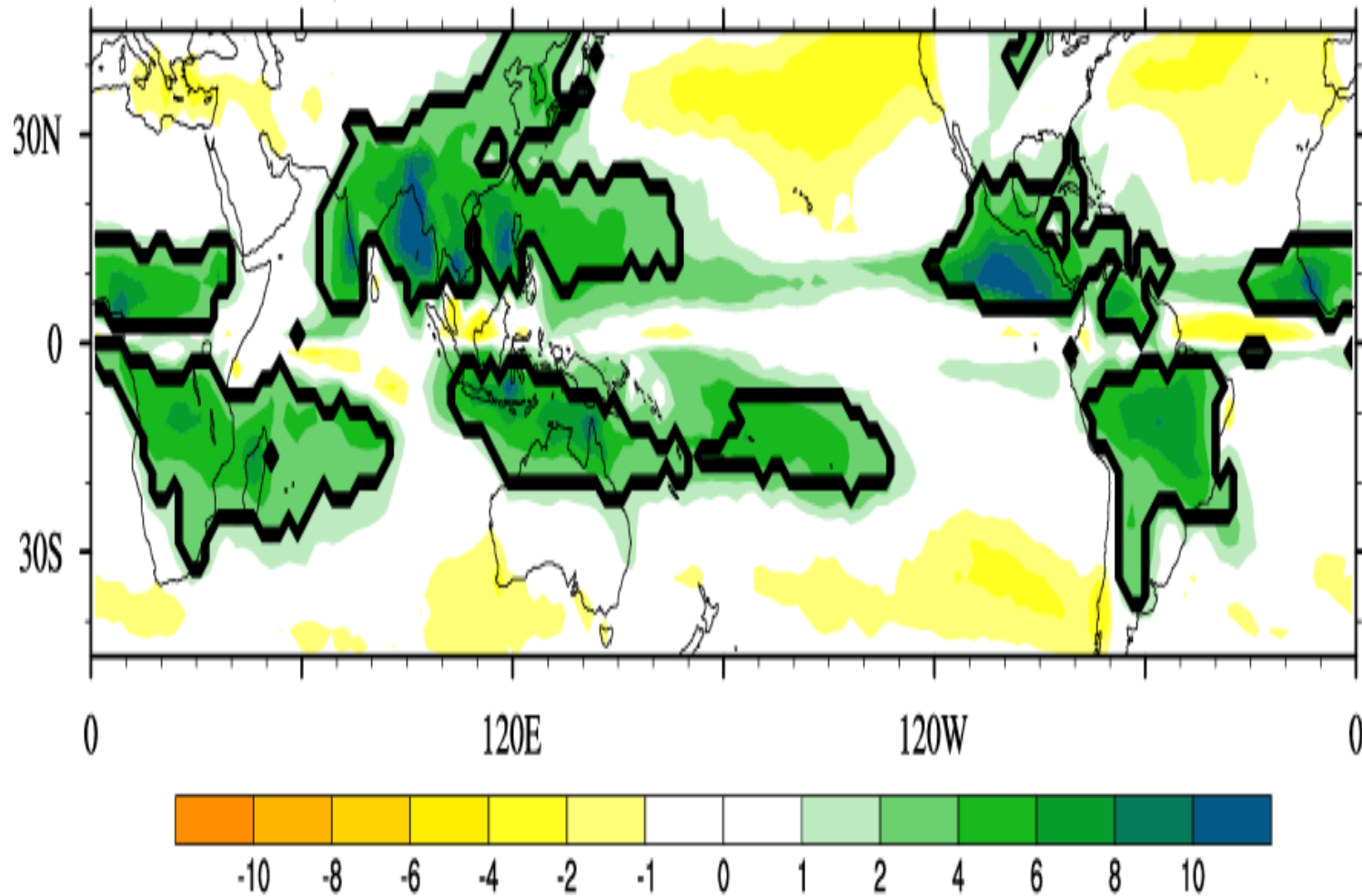
NHMI: NH-JJA “monsoon” precipitation

SHMI: SH-DJF “monsoon” precipitation

GMI: NHMI + SHMI

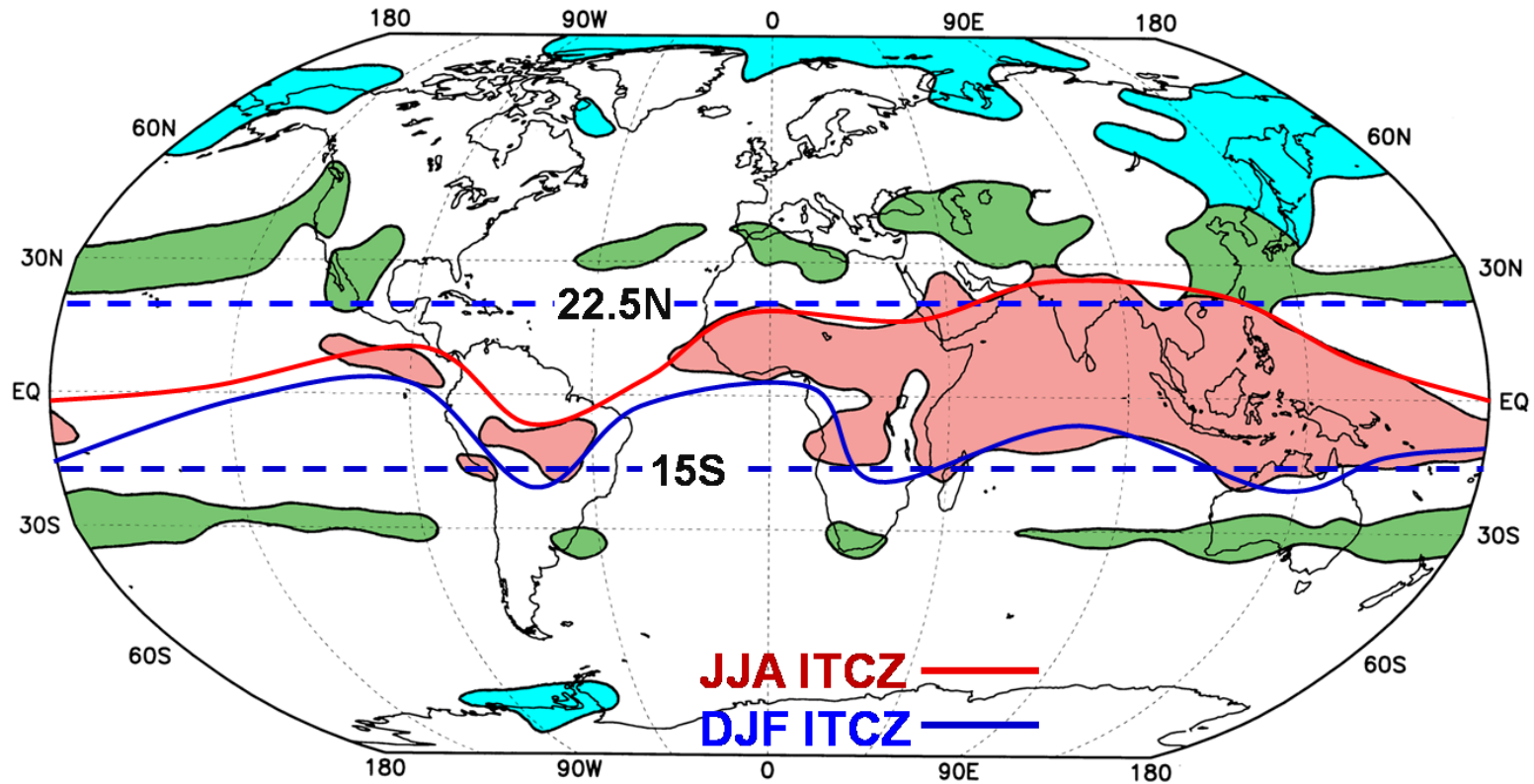
2. Monsoon Domain: **AR >180mm and >35% Total annual rainfall**

Global monsoon domains defined by rainfall



(Wang and Ding 2006 GRL)

Global monsoon domains defined by wind

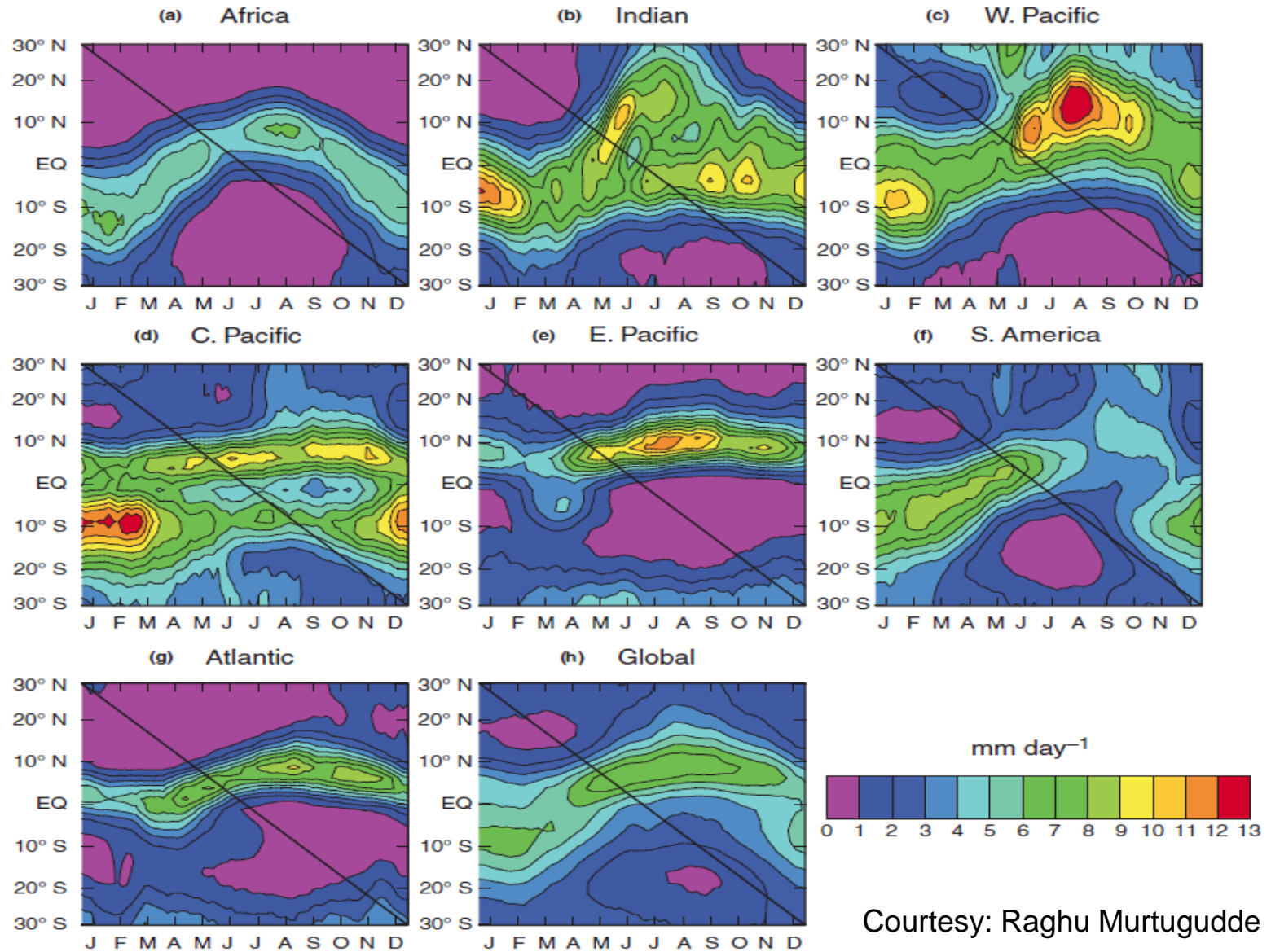


- tropical monsoon
- subtropical monsoon
- temperate-frigid monsoon

Defined based on wind

Li and Zeng (2003,2005)

Seasonal cycles of regional monsoon rainfall



Global monsoon changes

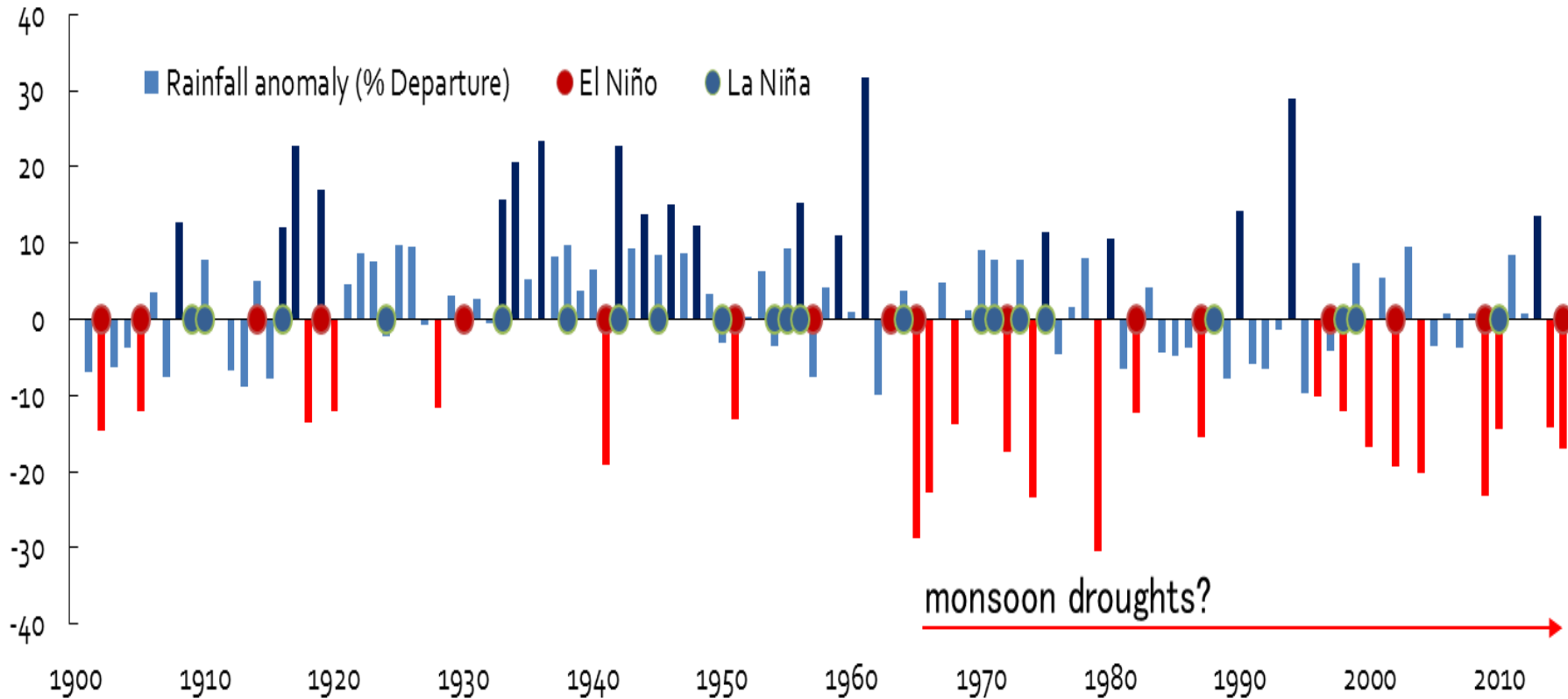
Photo by Fu Yunfei

Coordination among regional monsoons



- Each regional monsoon has its own characteristics due to its specific land-ocean configuration and orography, and due to differing feedback processes internal to the coupled climate system.
- There is coordination among regional monsoons: brought about by the annual cycle of the solar heating.
- There are connections in the global divergent circulation and thereby global monsoons: due to mass conservation.

The downward trend in the ISMR



The downward trend in the ISMR

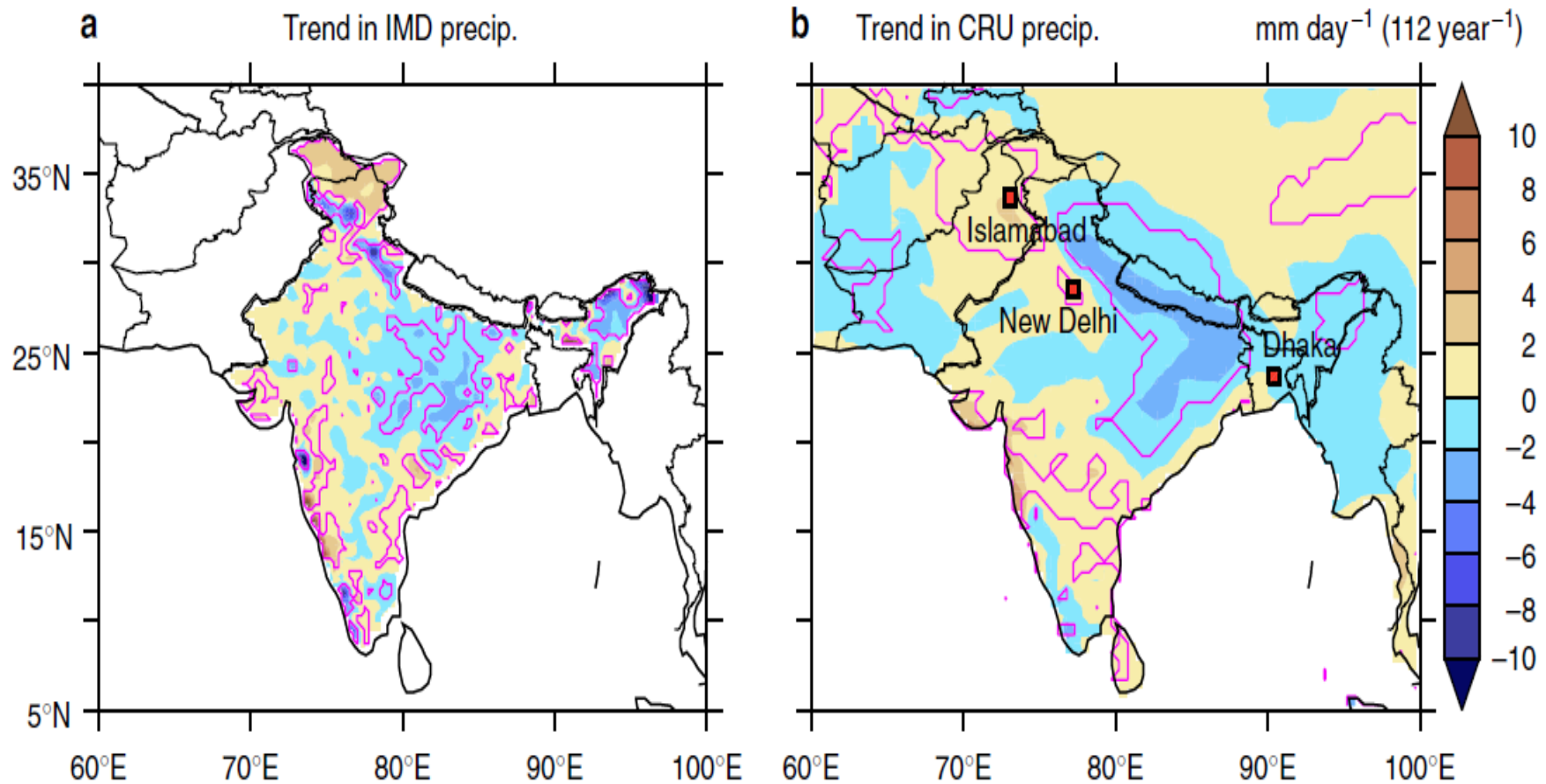
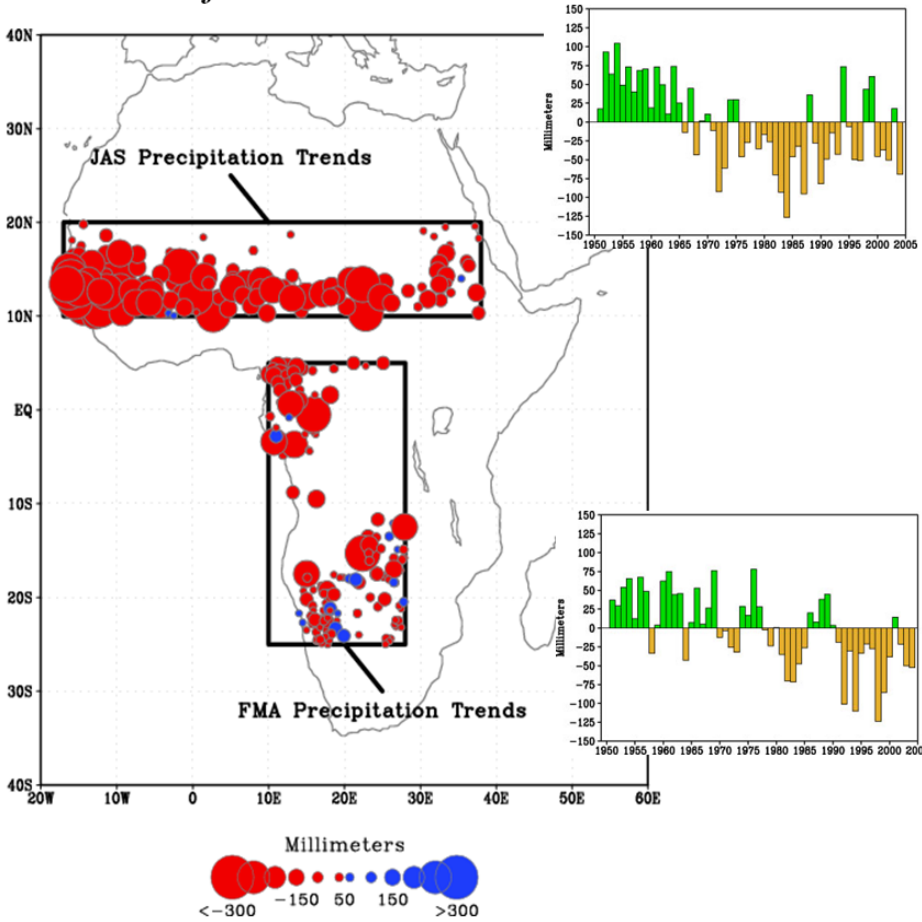


Figure 1 | Summer monsoon precipitation trends for the years 1901-2012. Observed trend in precipitation ($\text{mm day}^{-1} 112 \text{ year}^{-1}$) in (a) IMD and (b) CRU datasets, during June-September, for the years 1901-2012. Contours denote regions significant at the 95% confidence level.

Downward trends in East Asian and African monsoons

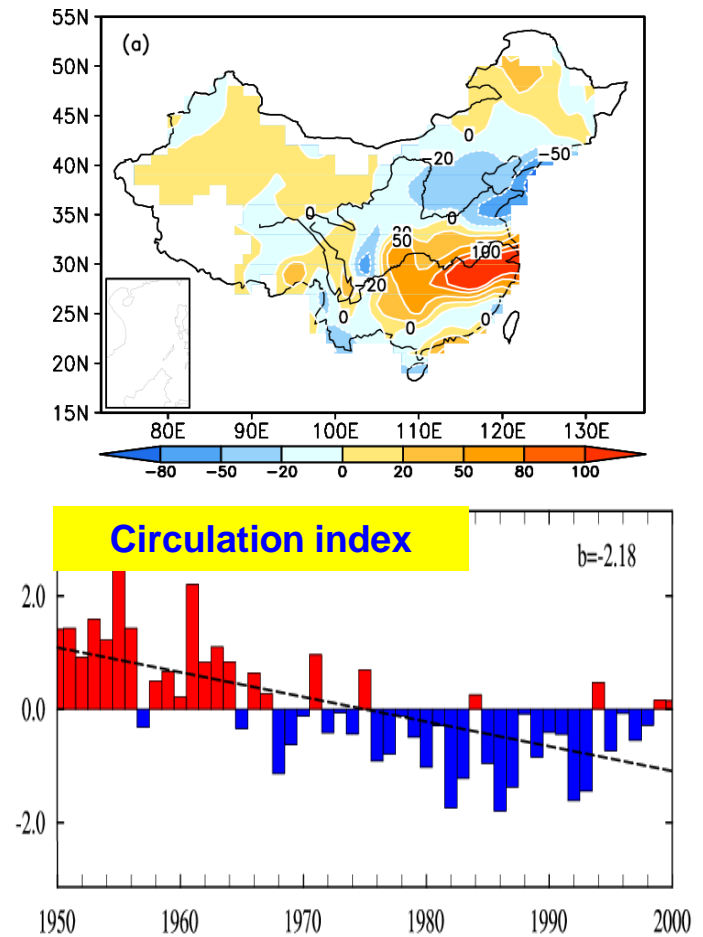


African rainfall



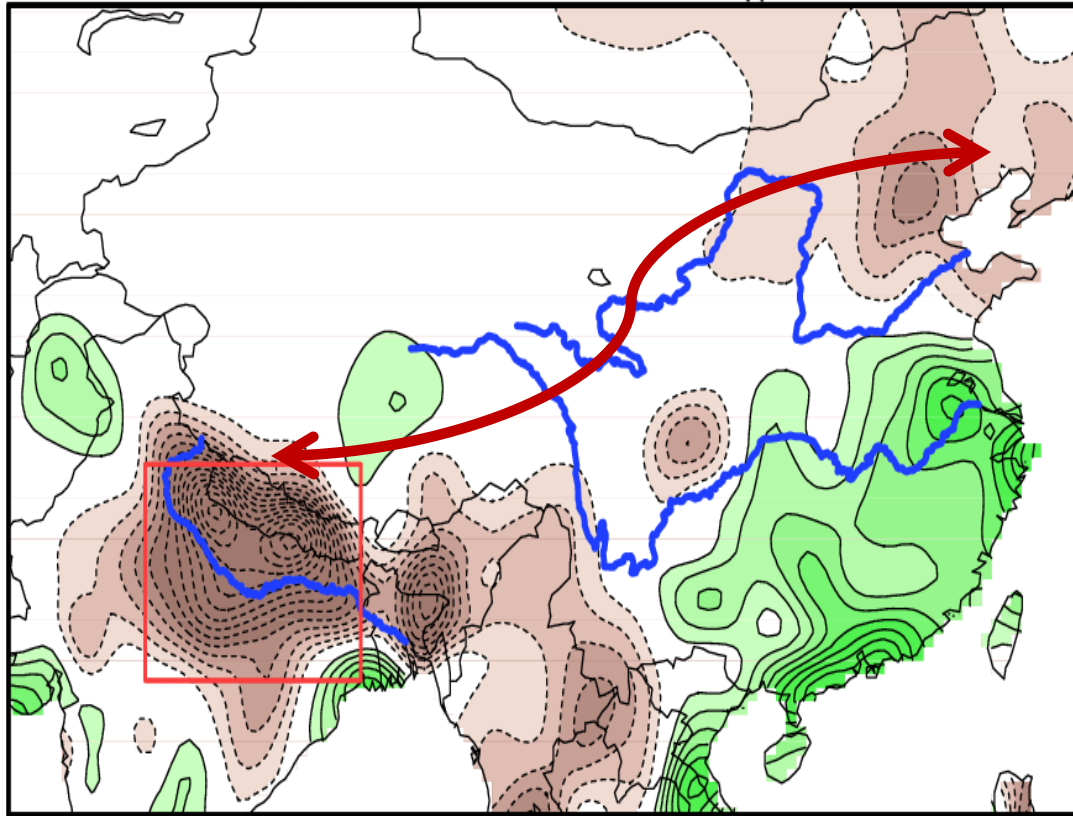
Hoerling et al. (2006) J. Climate

E Asian rainfall



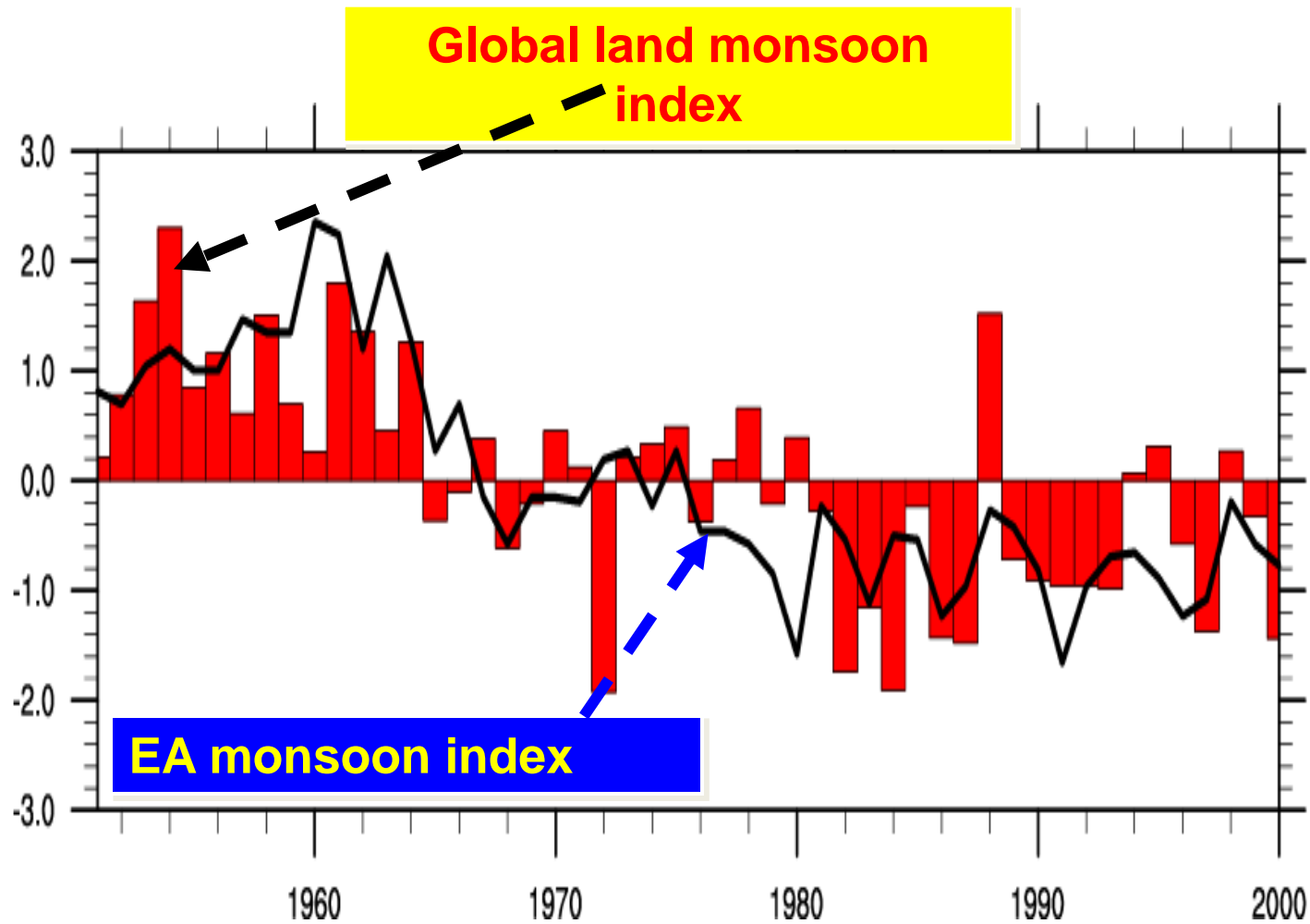
Zhou et al. (2009) Meteorologische Zeitschrift

Trends of S. Asia and E. Asia summer rainfall



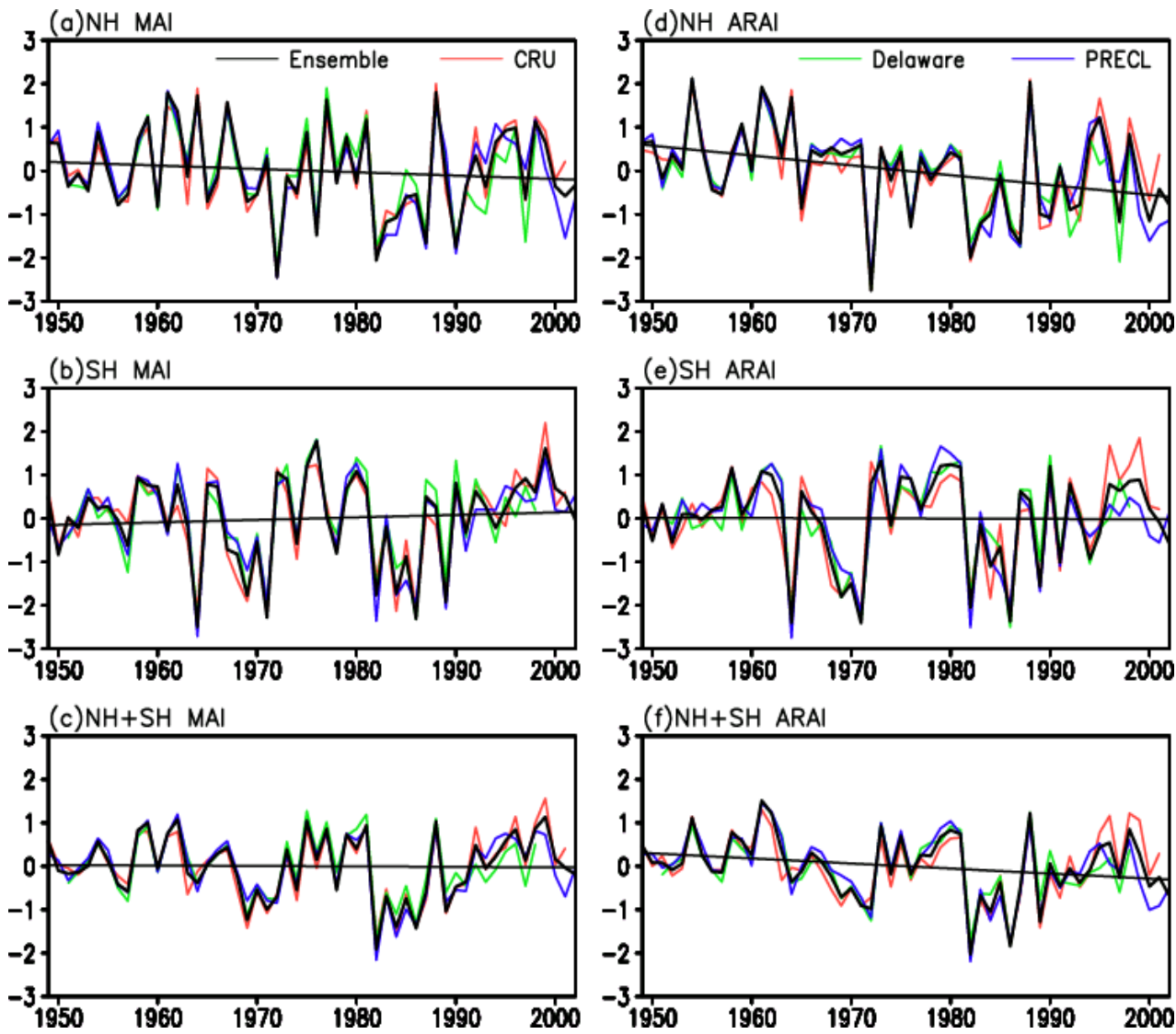
Linear trend in summer rainfall in the post--1950 period is plotted at 0.5 mm/day/century interval in the 0.5° resolution CRU TS 3.1 data; zero-contour is omitted. The South-Flood North-Dry pattern is manifest.

Changes of East Asian and global monsoon



Zhou T., L. Zhang, Hongmei LI 2008 Changes in global land monsoon area and total rainfall accumulation over the last half century, *Geophysical Research Letters*, 35, L16707, doi:10.1029/2008GL034881

Changes of land monsoon area and total rainfall (1948-2003)

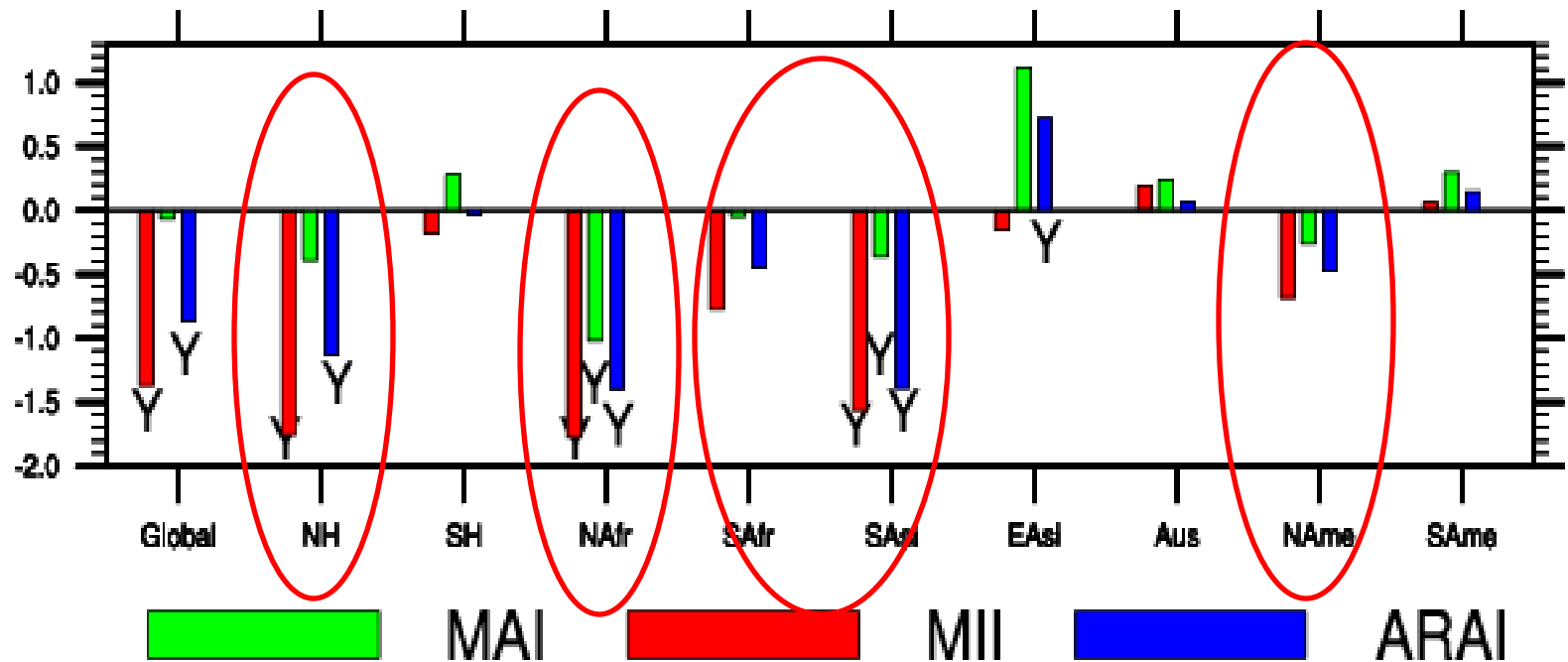


Zhou T, L. Zhang, and H. Li, 2008: **Changes in global land monsoon area and total rainfall accumulation over the last half century**, *Geophysical Research Letters*, 35, L16707, doi:10.1029/2008GL034881

Regional monsoon rainfall changes



Trends of monsoon rainfall **Area**, **intensity**, and **amount**
(1948-2003)



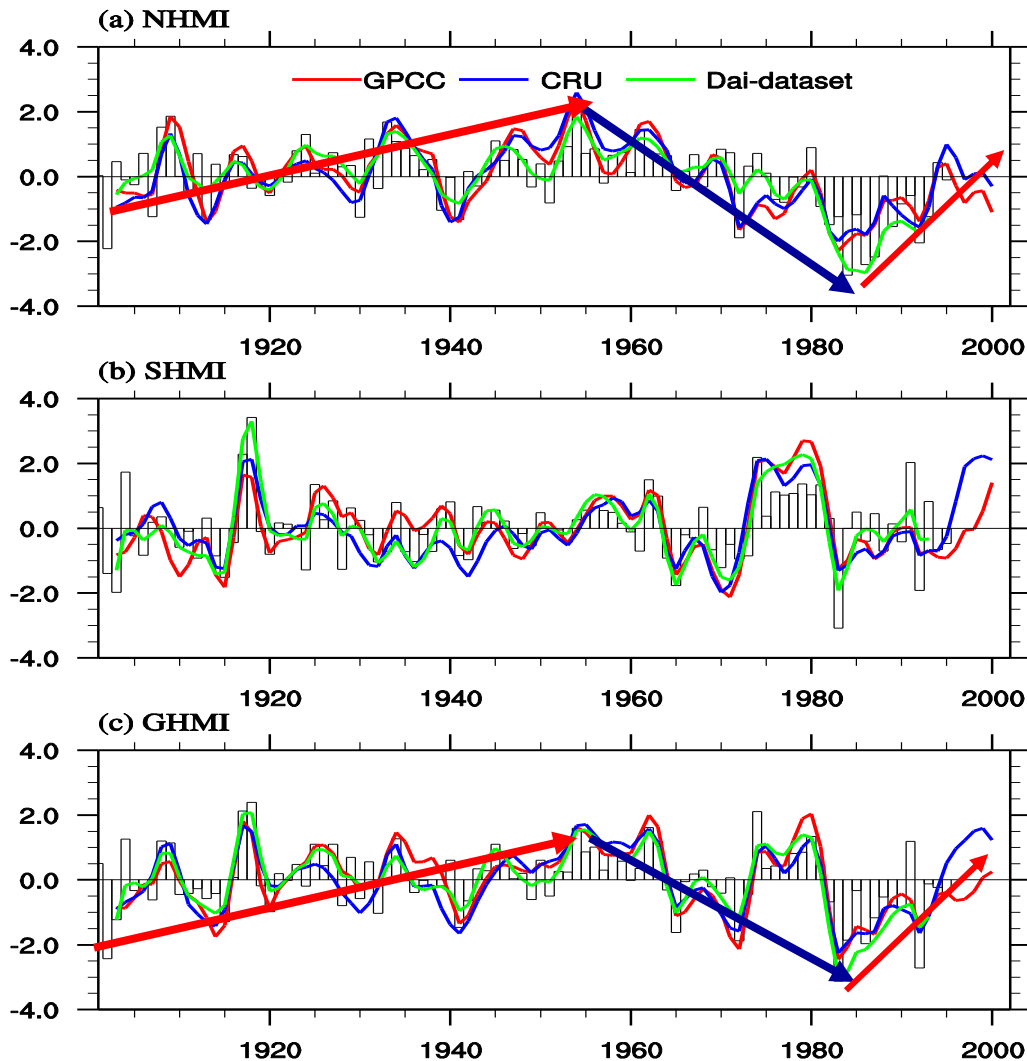
Monsoon Area

Intensity

Amount

(Zhou et al. 2008 Changes in global land monsoon area and total rainfall accumulation over the last half century, *Geophysical Research Letters*, 35, L16707, doi:10.1029/2008GL034881)

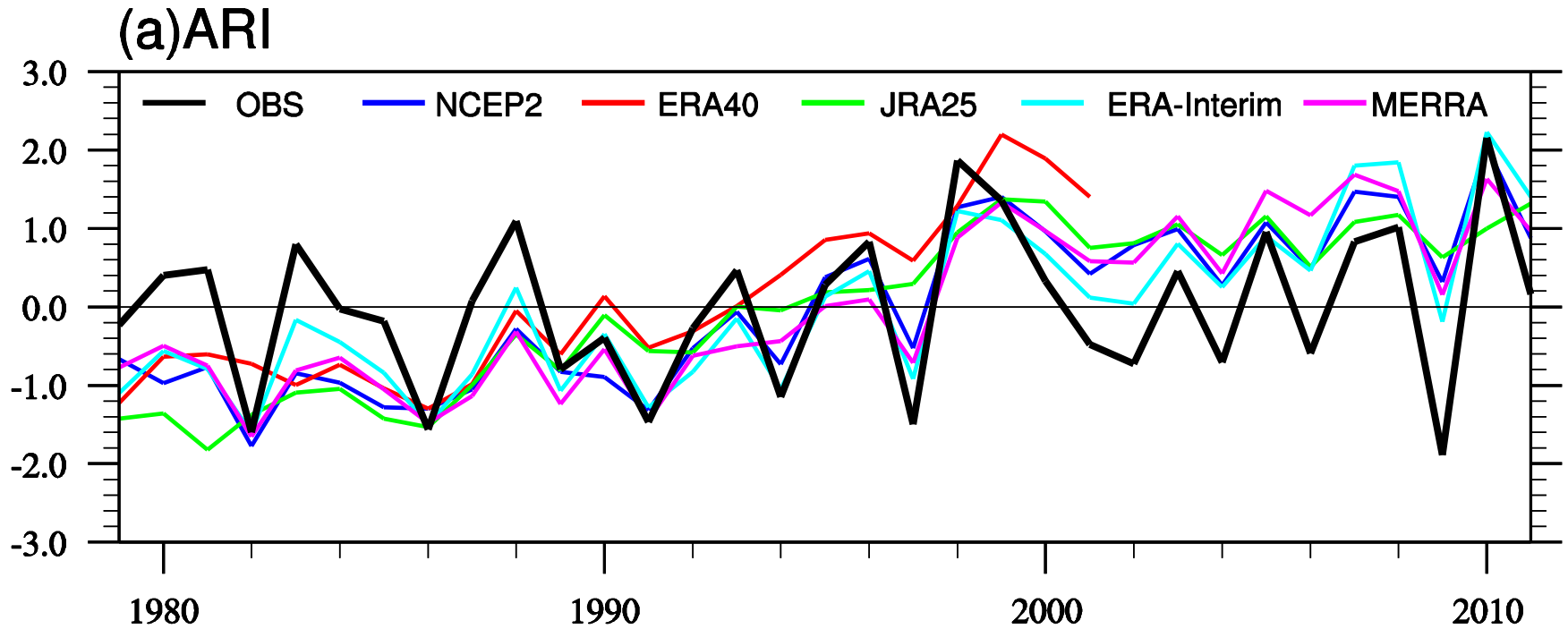
Changes of global land monsoon precipitation



Global and NH land monsoon:

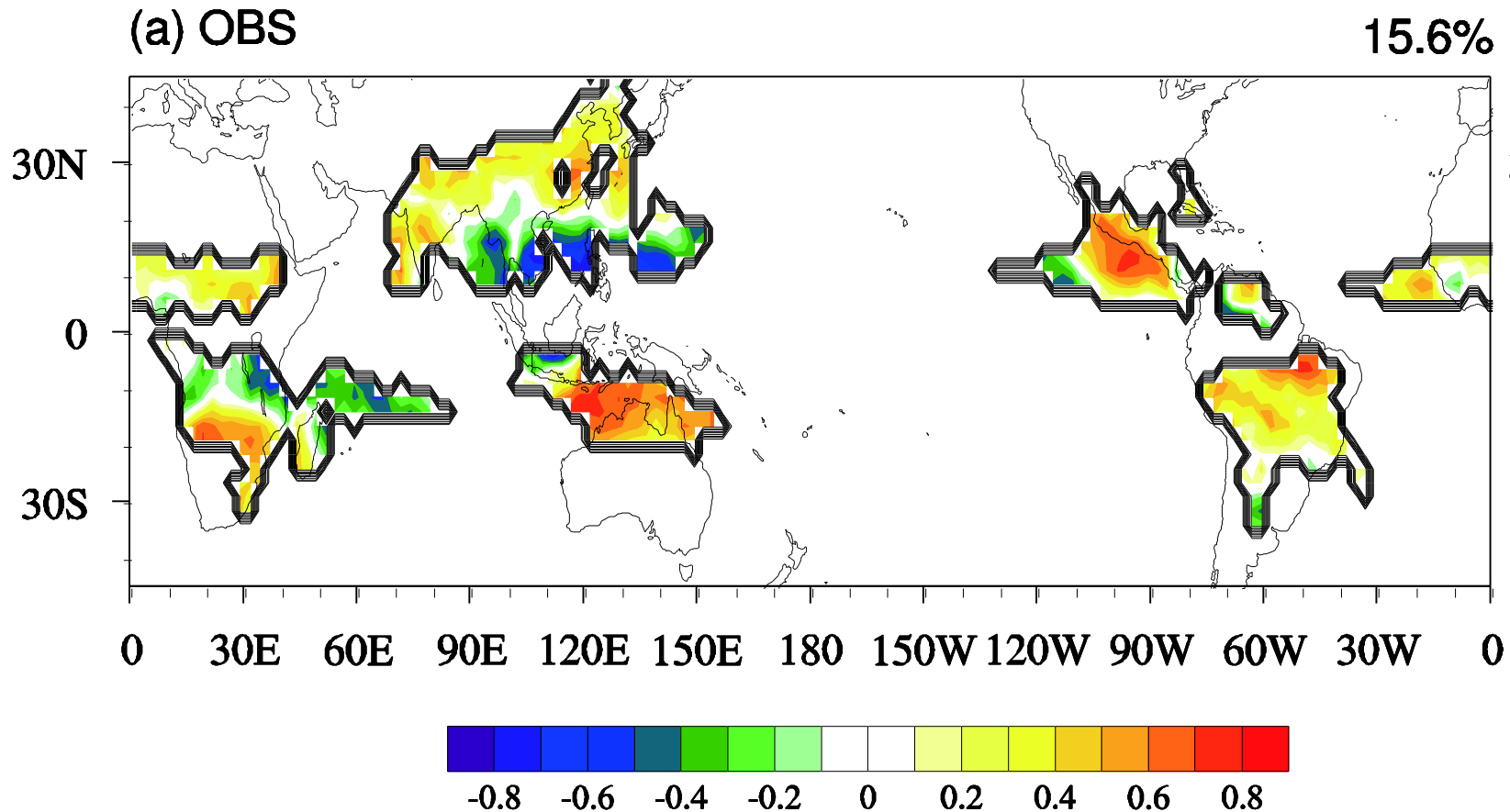
- 1) upward trend during 1901-1950s (95% confidence)
- 2) downward trend from 1950s to 1980s (95% confidence)
- 3) Recovering since the 1980s

EOF PC1 of GM precipitation



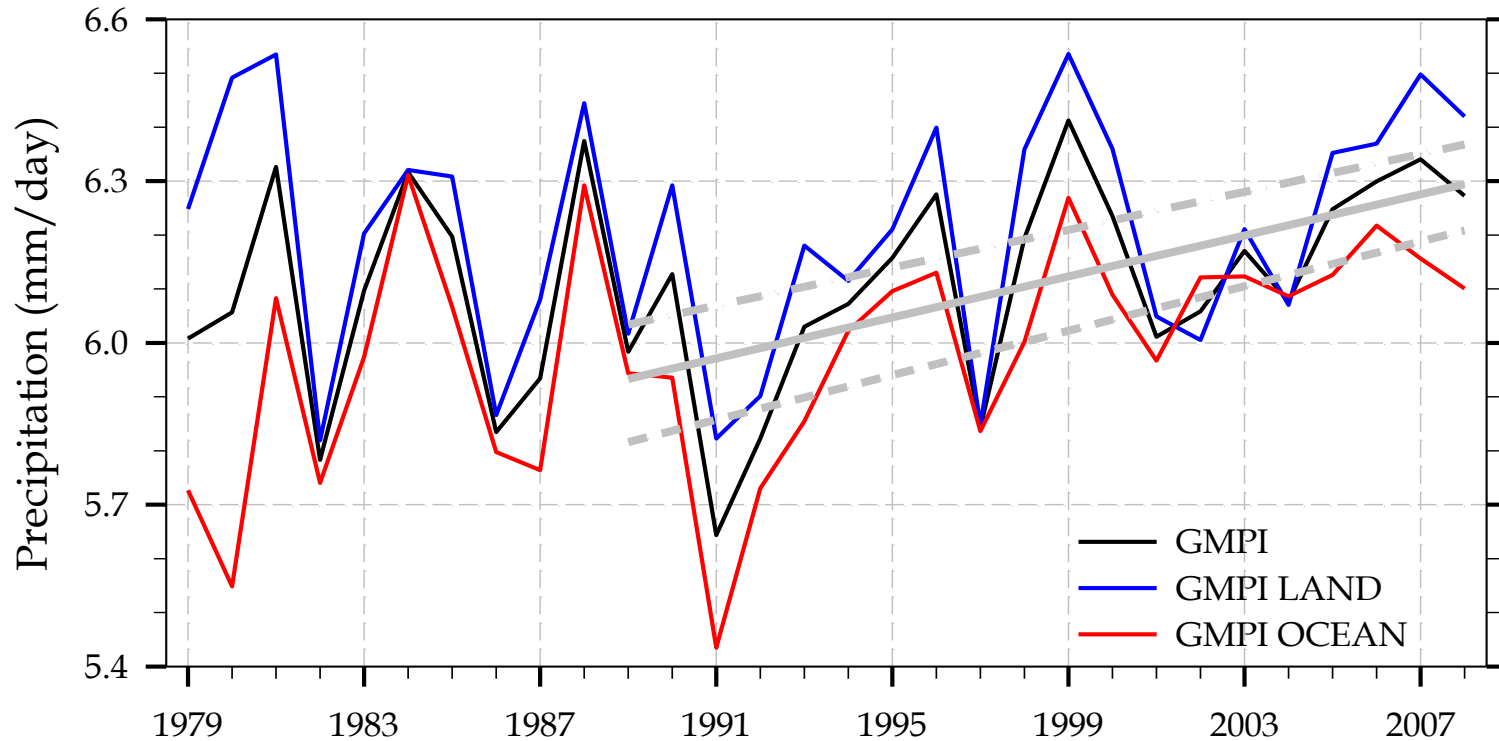
- The corresponding observational ARI shows increasing tendency **for 1979-2011**.
- All five reanalysis datasets show similar but stronger increasing trends than the observation.

Pattern of GM precipitation trends



- All five reanalysis can reproduce the observed positive anomalies in Australian monsoon region and northern part of Asian region.

Changes of global land monsoon precipitation



global land and ocean : upward trend for 1979-2009 (95% confidence level)

(Wang et al. 2012 Clim Dyn.)

Point # 1



- **The GM saw decadal variability in the 20th century, with a strengthening trend prior to the 1950s, a weakening trend during the 2nd half of the century.**
- **An enhanced trend of Global land monsoon is witnessed since the 1980s up to present.**



Outline

1. Background

2. Overview of GM

3. Responses to external forcings

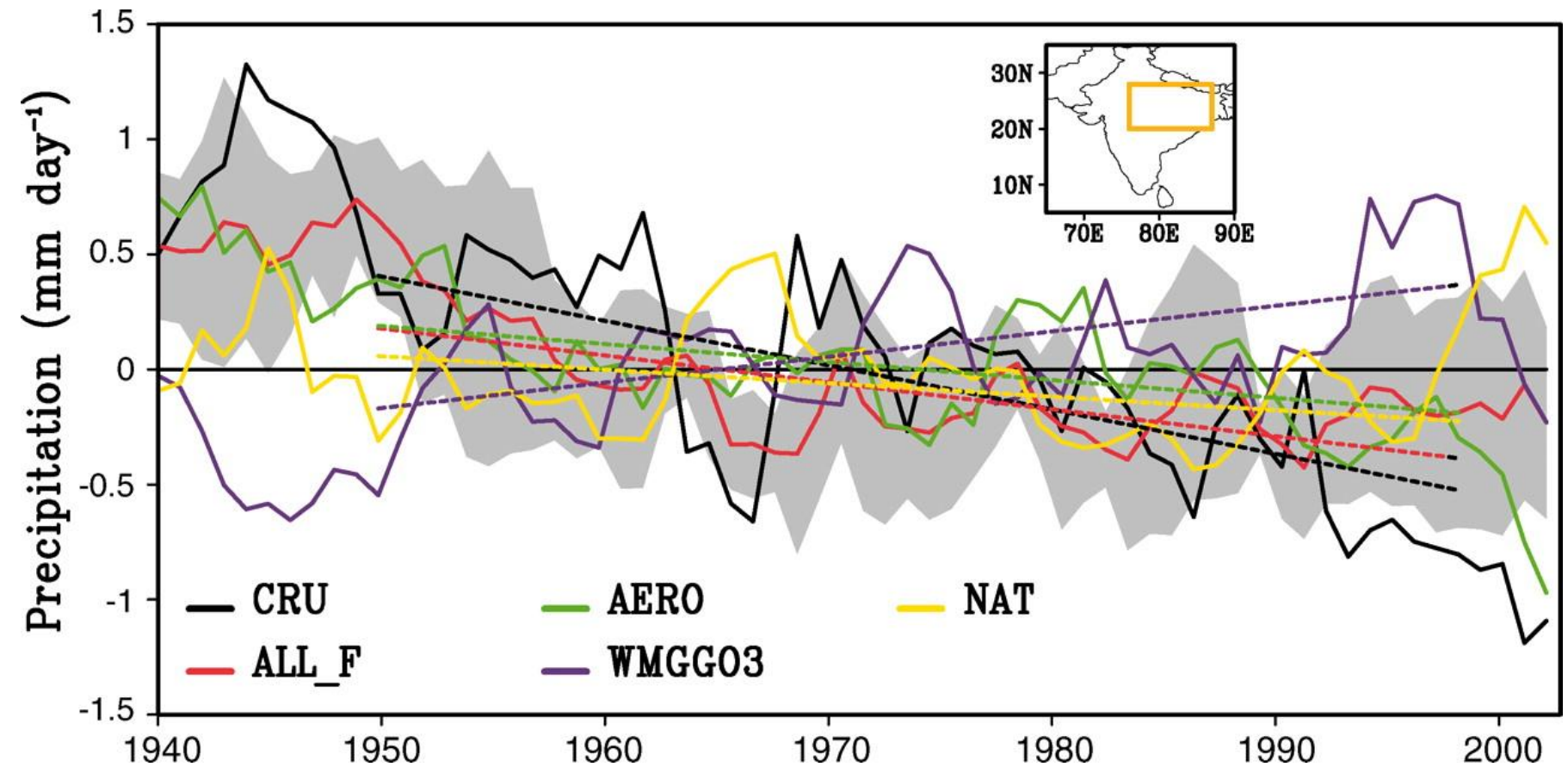
4. Concluding remarks



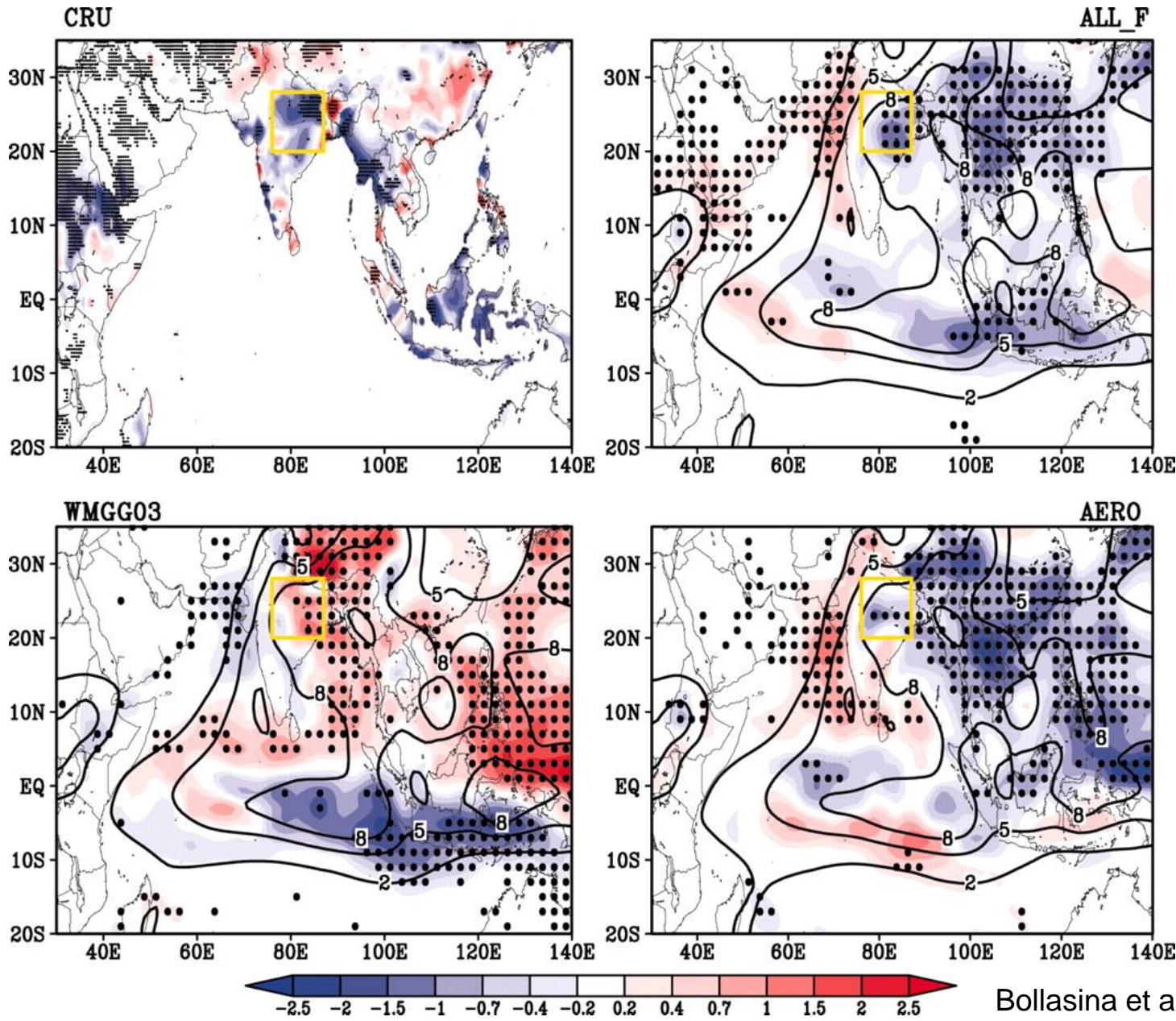
GHG & Aerosols

The image features a dramatic, high-contrast scene of industrial smokestacks. The sky is filled with thick, billowing plumes of smoke and aerosols, rendered in a palette of bright yellows, oranges, and deep reds, suggesting a sunset or sunrise. The smokestacks themselves are dark, silhouetted against the glowing background. The overall atmosphere is one of intense industrial activity and environmental impact.

Five-year running mean June-September average precipitation anomalies over central-northern India



The red, green, blue, and yellow lines are for the ensemble-mean all-forcing (ALL_F), aerosol-only (AERO), greenhouse gases and ozone-only (WMGG03), and natural forcing-only (NAT) CM3 historical integrations, respectively.



Point # 2



- ◆ Observations show that South Asia underwent a widespread summertime drying during the second half of the 20th century, but it is unclear whether this trend was due to natural variations or human activities.
- ◆ A series of climate model experiments is used to investigate the South Asian monsoon response to natural and anthropogenic forcings. The observed precipitation decrease can be attributed mainly to human-influenced aerosol emissions.
- ◆ The drying is a robust outcome of a slowdown of the tropical meridional overturning circulation, which compensates for the aerosol-induced energy imbalance between the Northern and Southern Hemispheres.
- ◆ These results provide compelling evidence of the prominent role of aerosols in shaping regional climate change over South Asia.

A satellite view of the Earth showing the East Asian continent, including China, Korea, and Japan, as well as the surrounding oceans and the Indonesian archipelago. The text "How about the East Asian summer monsoon?" is overlaid on the image, following the curve of the Earth's horizon.

How about the East Asian summer monsoon ?



The details of 17 CMIP5 models

No.	Model	Institute	Atmospheric resolution (lat*lon)	Member (35)
1	bcc-csm1-1	BCC/China	64*128	1
2	BNU-ESM	BNU/China	64*128	1
3	CanESM2	CCCma/Canada	64*128	5
4	CCSM4	NCAR/USA	192*288	3
5	CNRM-CM5	CNRM-CERFACS/France	128*256	6
6	CSIRO-Mk3-6-0	CSIRO-QCCCE/Australia	96*192	1
7	FGOALS-g2	IAP-THU/China	60*128	1
8	GFDL-CM3	NOAA GFDL/USA	90*144	1
9	GFDL-ESM2M	NOAA GFDL/USA	90*144	1
10	GISS-E2-H	NASA-GISS/USA	90*144	1
11	GISS-E2-R	NASA-GISS/USA	90*144	1
12	HadGEM2-ES	MOHC/UK	144*192	4
13	IPSL-CM5A-LR	IPSL/France	96*96	3
14	MIROC-ESM	MIROC/Japan	64*128	3
15	MIROC-ESM-CHEM	MIROC/Japan	64*128	1
16	MRI-CGCM3	MRI/Japan	160*320	1
17	NorESM1-M	NCC/Norway	96*144	1

Song F., T. Zhou, and Y. Qian, 2013: Responses of East Asian summer monsoon to natural and anthropogenic forcings in the 17 latest CMIP5 models. *Geophysical Research Letters*, 10.1002/2013GL058705

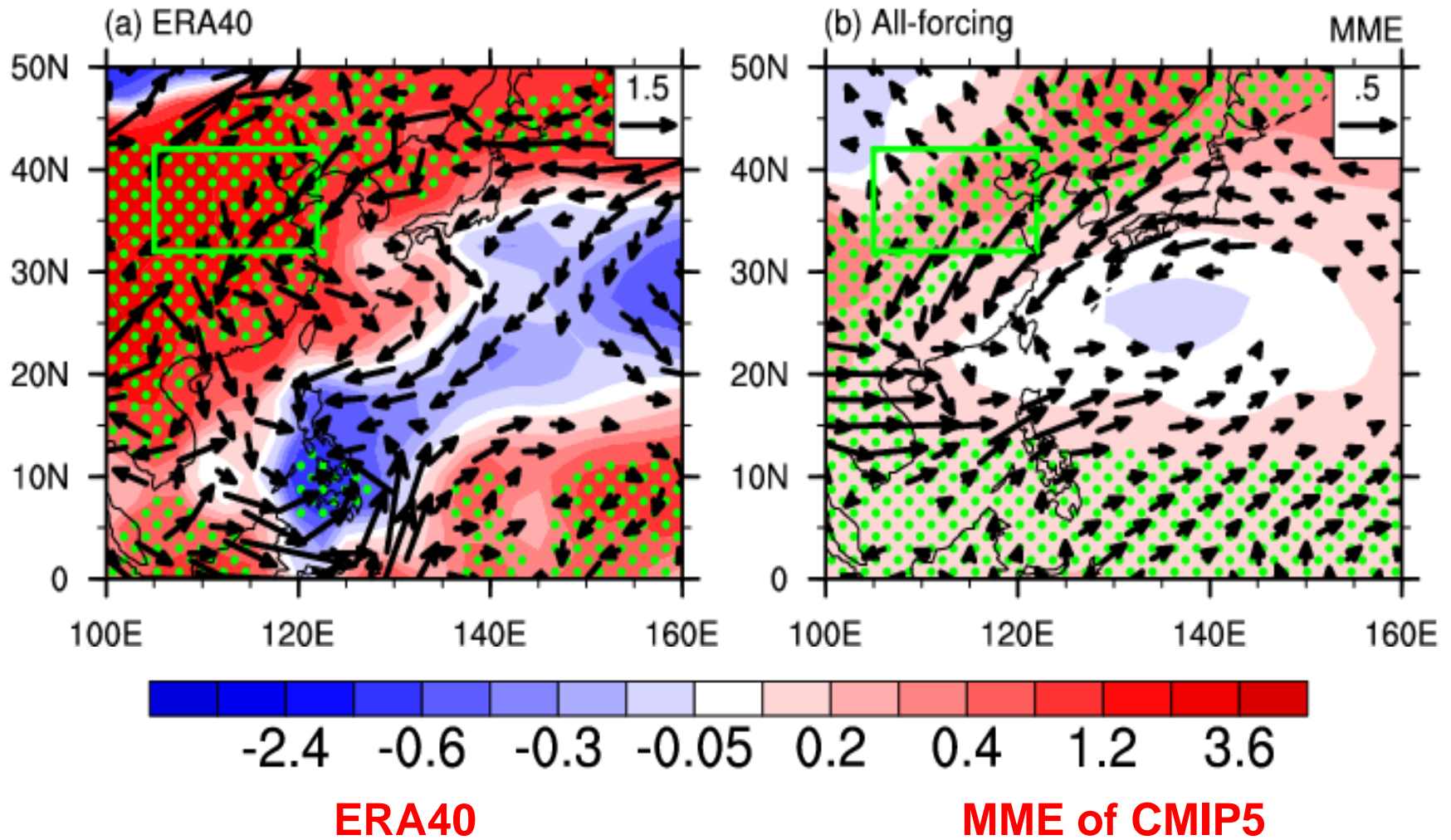
Details of three sets of CMIP5 experiments



Experiment description	CMIP5 label	Major purposes	Short name
Past ~1.5 centuries (1850–2005)	historical	Evaluation	All-forcing
historical simulation but with GhG forcing only	historicalGHG	Detection and attribution	GHG-forcing
historical simulation but with natural forcing only	historicalNat	Detection and attribution	Natural- forcing

- According to Taylor et al. (2009), **anthropogenic-forcing** is estimated by **All-forcing run minus Natural-forcing run**.
- **Aerosol-forcing** is estimated by **Anthropogenic-forcing run minus GHG-forcing run**. 105 realizations are analyzed.

Linear trends of SLP and 850 hPa winds (1958-2001)

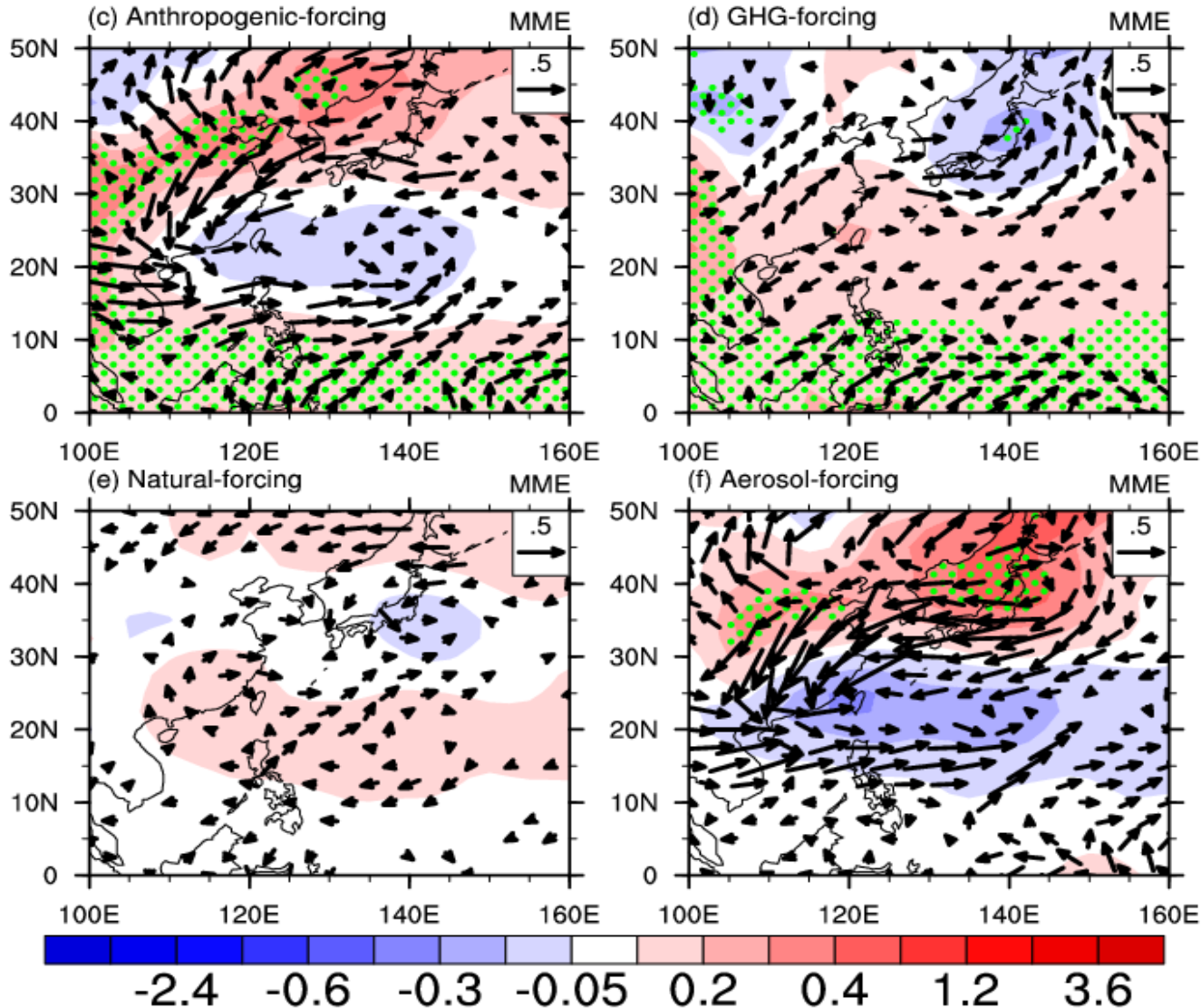


Song F., T. Zhou, and Y. Qian, 2013: Responses of East Asian summer monsoon to natural and anthropogenic forcings in the 17 latest CMIP5 models. *Geophysical Research Letters*, 10.1002/2013GL058705

Linear trends of SLP and 850 hPa winds (1958-2001)



**ALL
forcing**



**GHG
forcing**

**Natural
forcing**

**Aerosol
forcing**

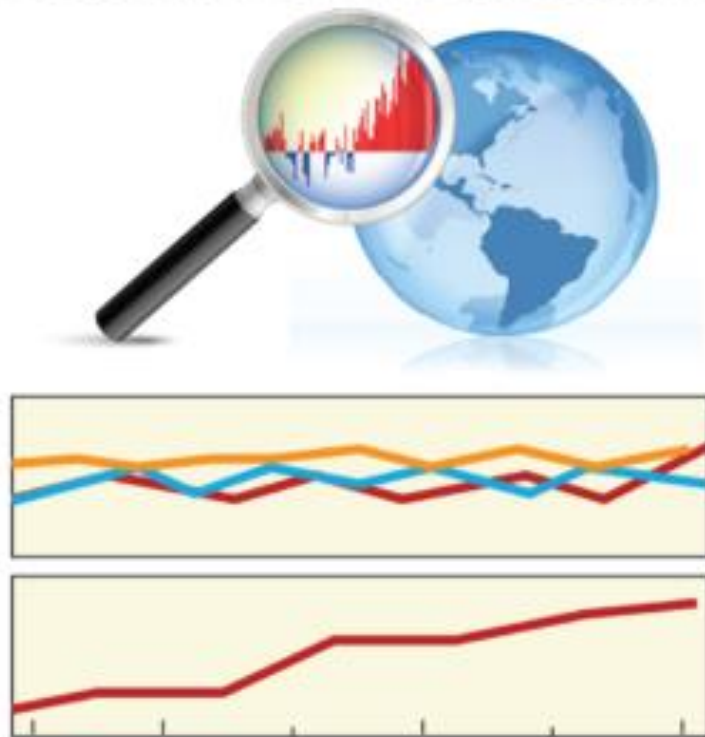
Point # 3



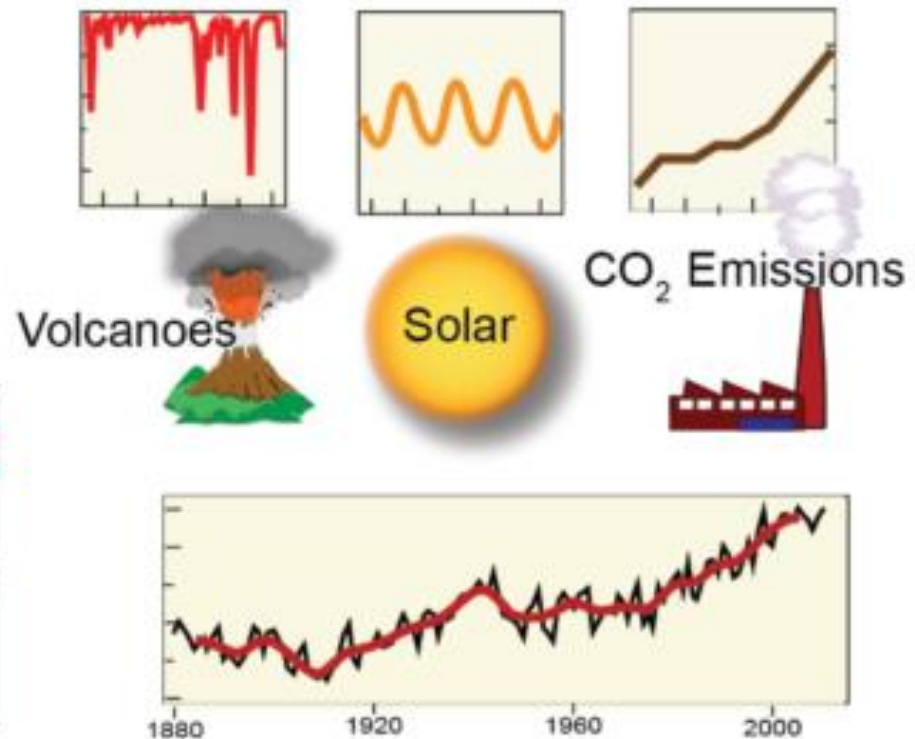
- ◆ The observed weakening trend of low-level EASM circulation during 1958–2001 is partly and weakly reproduced under all-forcing runs. A comparison of separate forcing experiments reveals that the aerosol forcing plays a primary role in driving the weakened low-level monsoon circulation.
- ◆ The preferential cooling over continental East Asia caused by aerosol affects the monsoon circulation through reducing the land-sea thermal contrast and results in higher sea level pressure over northern China.
- ◆ The increasing GHG forcing is favorable for an enhanced monsoon circulation.
- ◆ The models still failed in the simulation of monsoon rainband changes.



Detection and Attribution as Forensics



Detection: finding something out of the ordinary – a “signal” emerging from the noise



Attribution: determining the cause of the detected trend

Observation and Model Data



- ◆ **Observation:** daily Rain-gauge data from CMA
- ◆ **CMIP5 20c historical climate simulation:**
 - ✓ **ALL** forcing run :11 models, 54 ensemble members
 - ✓ **ANT**thropogenic foring: 6 models,26 members
 - ✓ **GHG** forcing: 10 models,34 members
 - ✓ **AA** forcing: 8 models, 22 members
 - ✓ **NAT**ural forcing: 11 models,37 members
 - ◆ **PI**control: 10 models, ~ 6000 yrs

Optimal fingerprinting Method

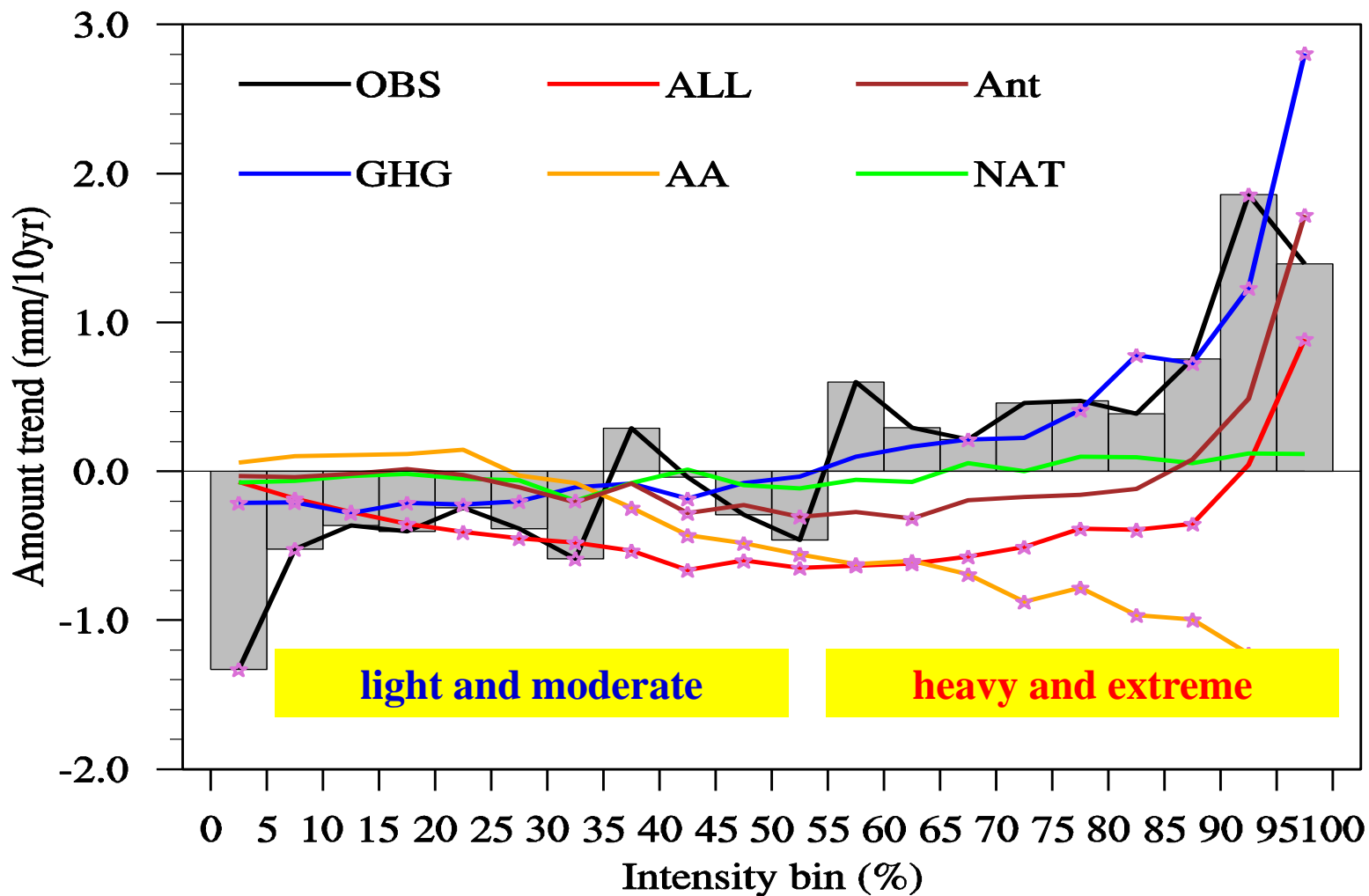


Optimal fingerprinting--Total least squares detection method

$$y = \sum_{i=1}^m (X_i - v_i) \beta_i + v_0$$

- **y**, observed trend, a rank-n vector, where n is the number of daily precipitation intensity bins, with n=20 used in this analysis;
- **X**, fingerprints or anomalous signals, model simulated climate responses to external forcings, a matrix with one column for each external climate forcing;
- **v_i**, **sampling noise**, estimated from the preindustrial control simulations and intra-ensemble differences;
- **v₀**, noise in the observations
- **β**, **scaling factors**, **inconsistent with 0 indicate a detectable signal, consistent with 1, then the model-simulated response patterns are consistent with the observed changes.**

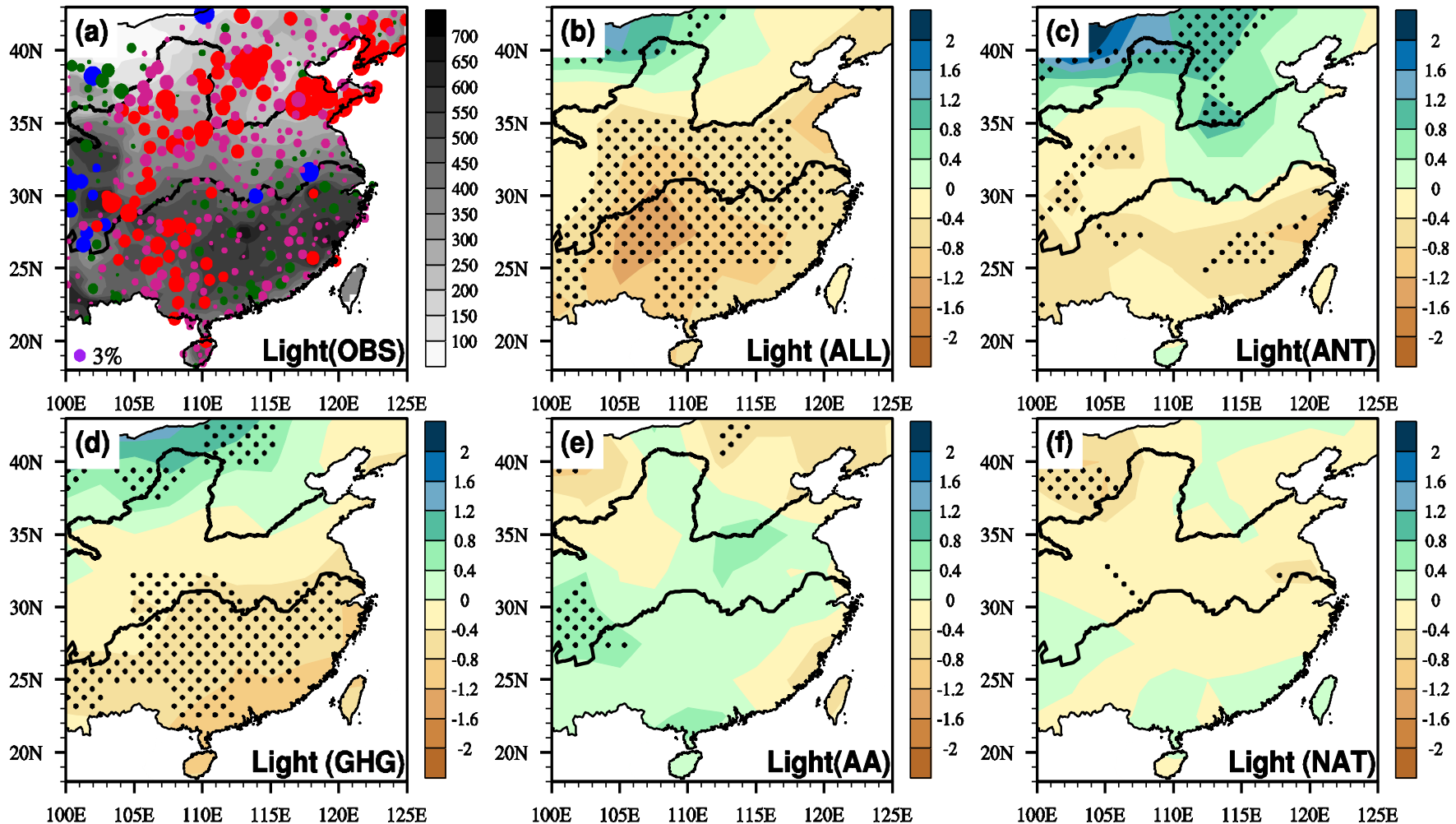
Trend of PDF in precipitation amount



Observation: a shift toward heavier precipitation

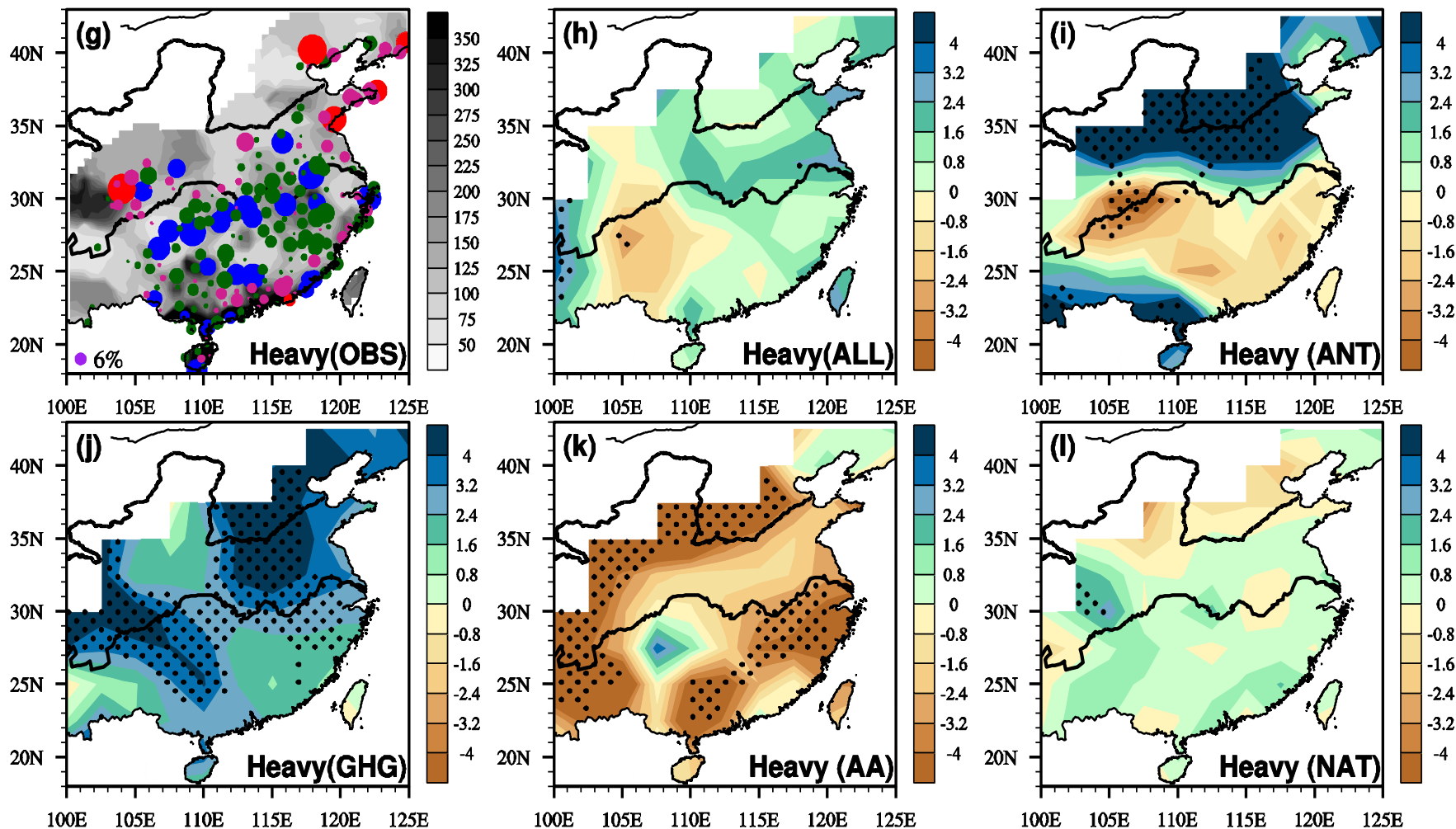
Simulation: The observed shift is well simulated with anthropogenic forcings.

Linear trends of light precipitation



The observed decrease in light precipitation mainly come from the contribution of GHG forcing. Anthropogenic aerosols partly offset the contribution of the GHGs.

Linear trends of heavy precipitation

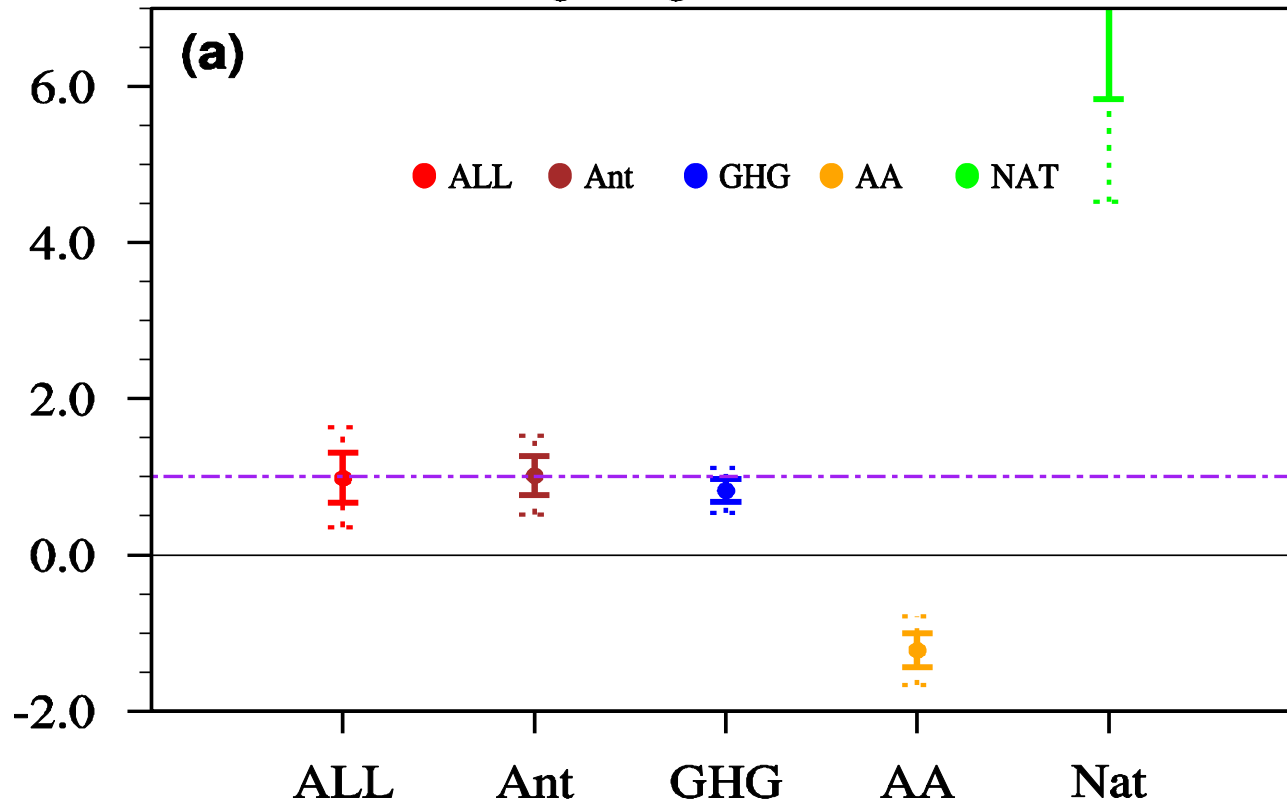


The observed increase of heavy precipitation is dominated by the GHG forcing.

Optimal detection



Single-signal Detection



Solid symbols: best estimates of regression coefficients (β);

Solid error bars: 5-95% uncertainty ranges of β ;

Dashed error bars: 5-95% uncertainty ranges of β when the internal variability is doubled.

- ANT forcing determines the forced changes in the ALL forcing run.
- The detected responses in ALL and ANT forcing runs are dominated by GHG forcing.

Point # 4

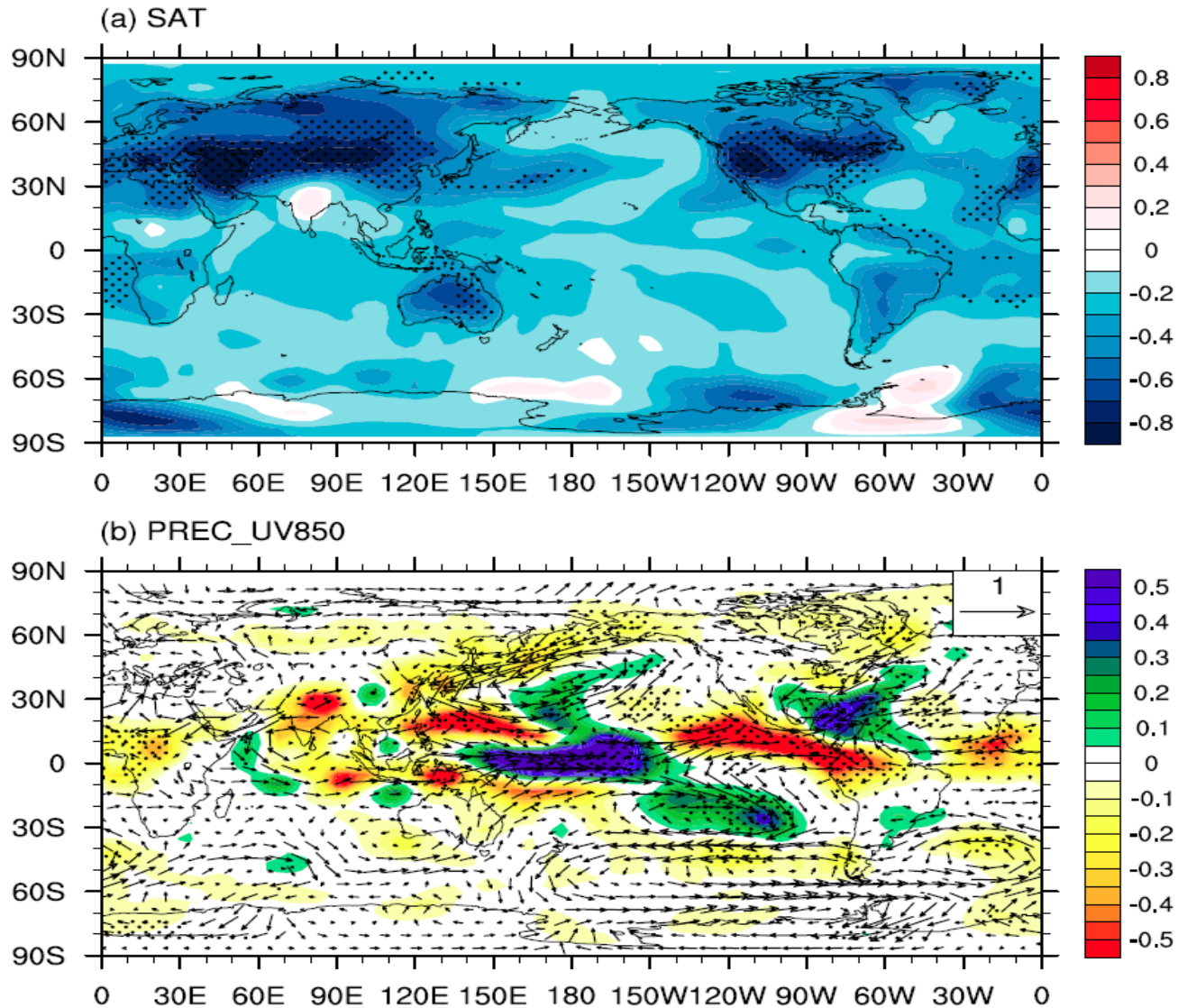


- ◆ The anthropogenic forcing has a detectable and attributable influence on the amount distribution of daily precipitation over EC during the second half of the 20th century.
- ◆ The observed shift from weak precipitation to intense precipitation is due primarily to the contribution of GHG forcing, with AA forcing offsetting some of the effects of the GHG forcing.
- ◆ Increasing of moisture and changes of monsoon circulation , resulting mainly from GHG-induced warming, favors heavy precipitation over eastern China.

A dramatic photograph of a volcanic eruption. A thick, dark grey plume of ash and smoke billows upwards from a dark, rocky volcanic landscape. The plume is dense and textured, with a large, rounded top. The sky is a mix of blue and grey, suggesting a hazy or overcast day. The foreground shows the dark, jagged peaks of the volcano, with some white steam or smoke rising from the lower slopes.

Volcanic aerosols

Summer climate after large volcanic eruptions



The image is a composite graphic. On the left side, there is a dark silhouette of an industrial factory with a tall chimney emitting a thick plume of dark smoke. The background behind the factory is a fiery orange and red sky. On the right side, there is a satellite-style view of the Earth, showing the continents of Africa, Europe, and parts of Asia. The Earth is set against a bright yellow and orange glow that transitions into the fiery sky on the left. The text "Changes under Global warming" is written in a bold, white, sans-serif font across the center of the image, overlapping both the factory and the Earth.

Changes under Global warming

Global Monsoon: Area (GMA)

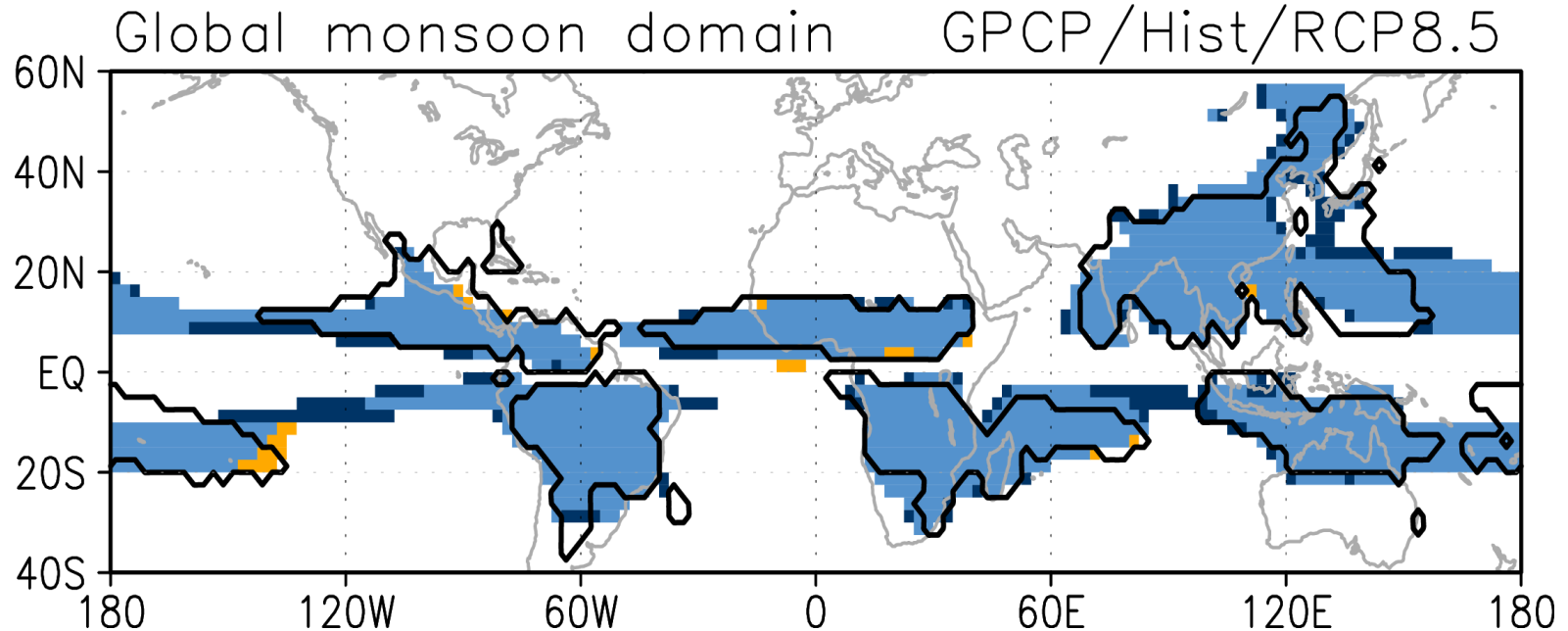


Black Contour: GPCP

Shading: MME of 29 CMIP5 models

Yellow shading: only in present

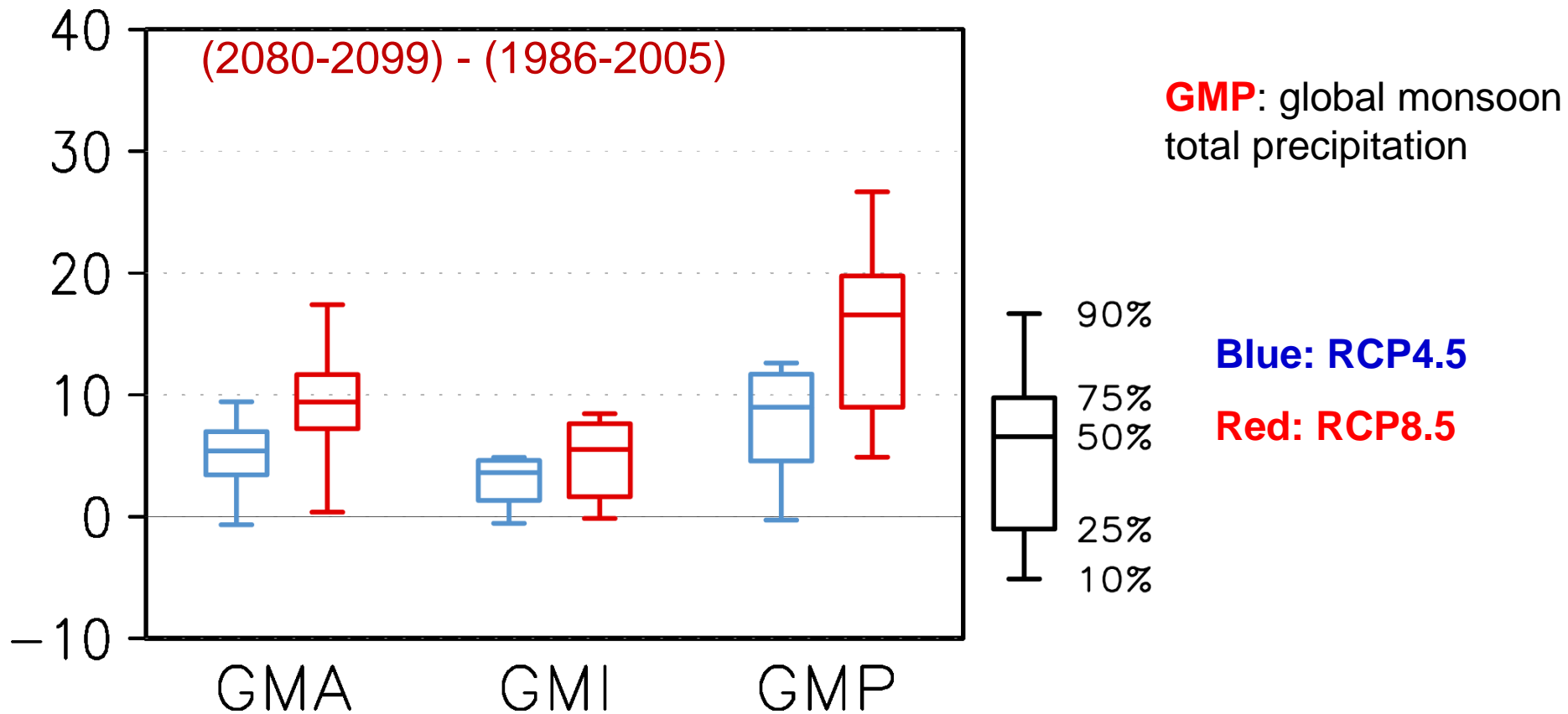
Dark blue: only in future



The global monsoon area will expand mainly over the central to eastern tropical Pacific, the southern Indian Ocean, and eastern Asia.



Future change (%): GMA, GMI & GMP

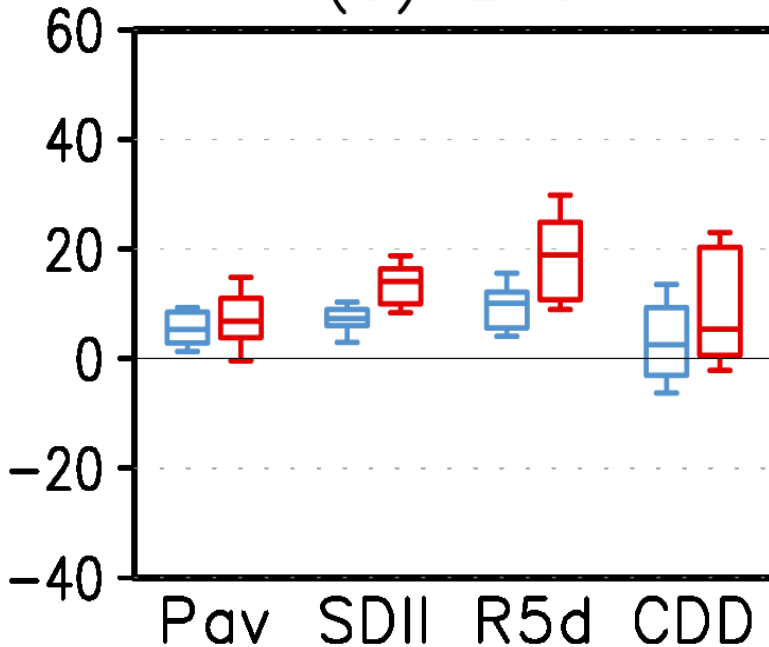


- GMP shows an increase in the RCP4.5 scenario and more so in the RCP8.5 scenario
- monsoon-related precipitation will significantly increase in a warmer climate

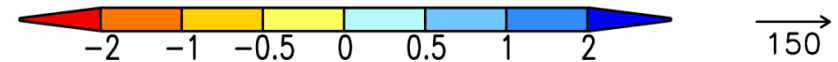
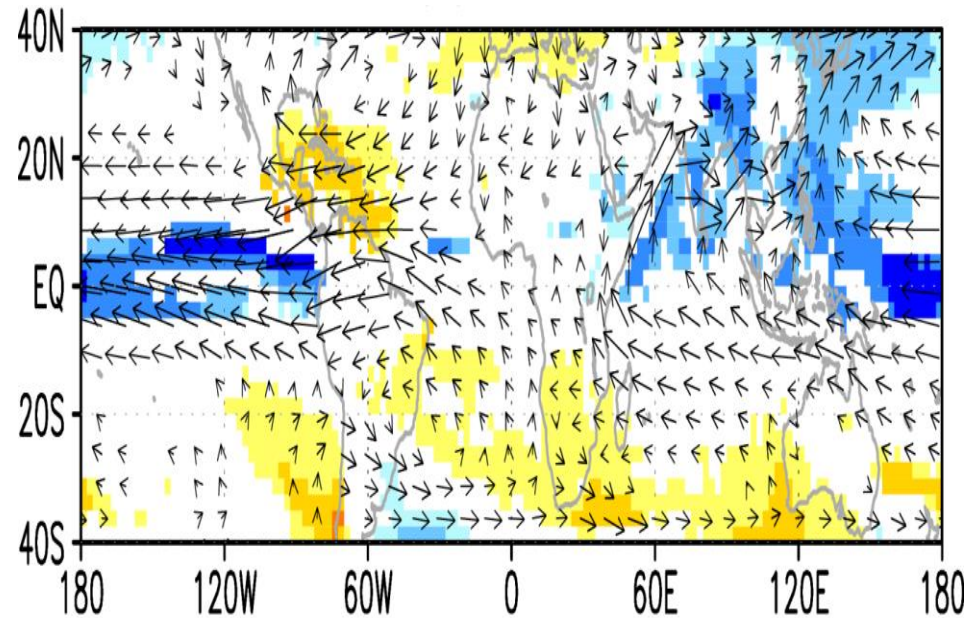
Future change ratio of Pav, SDII, R5d and DD over E. Asia



(b) EAS



Blue: RCP4.5 Red: RCP8.5



shading: Precipitation

vector: vertically integrated water vapor flux

Kitoh, A., H. Endo, K. Krishna Kumar, I. F. A. Cavalcanti, P. Goswami, and T. Zhou, 2013: Monsoons in a changing world: a regional perspective in a global context. *J. Geophys. Res. Atmos.*, 118, doi:10.1002/jgrd.50258

Point # 5



1. The global monsoon area defined by the annual range in precipitation *is projected to expand mainly* over the central to eastern tropical Pacific, the southern Indian Ocean, and eastern Asia.
2. The global monsoon precipitation *intensity* and the global monsoon *total precipitation* are also projected to increase. Indices of *heavy precipitation* are projected to *increase much more than those for mean precipitation*.
3. The projected increase of the global monsoon precipitation can be attributed to an *increase of moisture convergence due to increased surface evaporation and water vapor in the air column* although offset to a certain extent by the *weakening of the monsoon circulation*.



THANKS

<http://www.lasg.ac.cn/staff/ztj>